CHAPTER IV

RESULTS AND DISCUSSION

This chapter focused on the methodology of the synthesis and characterization of Schiff's base doped mesoporous silica. The amount of incorporated Schiff's base molecules was examined as an important factor. The influence of temperature on the synthesis was also determined. Various extraction factors of these modified sorbents to divers divalent cations were studied to search for the optimum extraction conditions.

4.1. Synthesis of Schiff's base

Four Schiff's base ligands such as salen, saltn, salophen and haen were prepared by slowly adding an interested aldehyde or ketone (2 mol-equiv.) to a solution of primary diamines (1 mol-equiv.) in methanol. The resulting mixture was stirred at room temperature until precipitate occurred. The solid was then filtered off, washed and recrystallized by an appropriate solvent. The type of starting substrate used for the synthesis of each Schiff's base was shown in Table 4.1.

Table 4.1 Starting substrate used for the synthesis of various Schiff's bases.

Type of Schiff's base	Type of starting substrate	
	aldehyde or ketone	diamine
Salen	salicylaldehyde	ethylenediamine
Saltn	salicylaldehyde	2-propylenediamine
Salophen	salicylaldehyde	*o*-phenylenediamine
Haen	2-hydroxyacetophenone	ethylenediamine

The physical properties of all obtained Schiff's bases were displayed as follows.

2,2'-{ethane-1,2-diylbis[nitrilo(*E*)methylylidene]}diphenol (salen): Bright yellow crystal 90% yield; m. p. 128-129 °C; IR (KBr): 3500 (w), 3010-3050 (w), 2860-2950 (w), 1790-2040 (w), 1635 (s), 1460-1610 (w), 1280 (s) and 1150 (s) cm^{-1}; ^{1}H-NMR ($CDCl_3$) δ (ppm): 3.99 (s, 4H), 6.90 (dt, J = 7.80, 2H), 6.97 (d, J = 8.58,

2H), 7.30 (dd, J = 1.64, 2H), 8.40 (s, 2H) and 13.2 (s, 2H); ^{13}C-NMR ($CDCl_3$) δ (ppm): 59.8 (2C), 117.0 (2C), 118.7 (2C), 131.5 (2C), 132.4 (2C), 160.9 (2C), 166.5 (2C).

2,2'-{propane-1,3-diylbis[nitrilo(*E*)methylylidene]}diphenol (saltn): Yellow needle crystal 28% yield; m. p. 52-53 °C; IR (KBr): 3500 (w), 3000-3060 (w), 2850-2950 (w), 1635 (s), 1627, 1580, 1500 (m), 1280 (m) and 750 (s) cm^{-1}; ^{1}H-NMR ($CDCl_3$) δ (ppm): 2.13-2.16 (quintet, 2H, J = 7.02), 3.74-3.76 (dt, J = 7.03), 6.90-7.37 (m, 8H), 8.42 (s, 2H) and 13.48 (s, 2H); ^{13}C-NMR ($CDCl_3$) δ (ppm): 31.7 (C), 56.8 (C), 117.0 (2C), 118.7 (2C), 118.7 (2C), 131.3 (2C), 132.4 (2C), 161.1 (2C) and 165.5 (2C).

2,2'-{1,2-phenylenebis[nitrilo(*E*)methylylidene]}diphenol (salophen): Orange needle crystal 75% yield; m. p. 168-169 °C; IR (KBr): 3502 (w), 3054 (w), 2980-2858 (w), 1619 (s), 1485-1560 (s), 1275 (s) and 1190 (s) cm^{-1}; ^{1}H-NMR ($CDCl_3$) δ (ppm): 6.95 (t, J = 7.81, 2H), 7.08 (d, J = 8.59, 2H), 7.28 (m, 4H), 7.38 (m, 2H), 7.43 (m, 2H), 8.68 (s, 2H) and 13.09 (s, 2H); ^{13}C-NMR ($CDCl_3$) δ (ppm): 117.6 (2C), 119.0 (2C), 119.2 (2C), 119.8 (2C), 127.8 (2C), 132.4 (2C), 133.4 (2C), 142.6 (2C), 161.4 (2C) and 163.7 (2C).

2,2'-{ethane-1,2-diylbis[nitrilo(1*E*)eth-1-yl-1-ylidene]}diphenol (haen): Yellow needle crystal 80% yield; m. p. 199-200 °C; IR (KBr): 3500 (w), 3010-3050 (w), 3070 (w), 2880-2940 (w), 1800-1920 (w), 1612 (s), 1440-1600 (s), 1240 (s) and 1180 (s) cm^{-1}; ^{1}H-NMR ($CDCl_3$) δ (ppm): 2.47 (s, OH), 4.06 (s, 4H), 6.85 (dt, J = 7.87, 1.29, 2H), 7.O2 (dd, J = 8.58, 1.29, 2H), 7.30 (dt, J = 7.98, 1.82, 2H), 7.56 (dd, J = 7.85, 1.49, 2H) and 12.31 (s, 2H); ^{13}C-NMR ($CDCl_3$) δ (ppm): 14.8 (2C), 50.2 (2C), 117.4 (2C), 118.5 (2C), 119.4 (2C), 128.2 (2C), 132.5 (2C), 163.0 (2C) and 173.0 (2C).

4.2. Synthesis of materials

4.2.1. Salen doped mesoporous silica

With the aim to gain the maximum amount of incorporated salen, the comparative study on the influence of temperature was conducted. Also, the quantity of salen used in the synthesis was varied for achieving the maximum amount of incorporated salen.

4.2.1.1. Preliminary study

To attain an appropriate synthesis condition, the preparation of salen doped mesoporous silica was performed according to method I at two different temperatures, 40 ºC and 60 °C. In both cases, after the synthesis procedure, the resulting yellowish silica was observed. However, the pale yellow supernatant and washing solutions were obtained due to the existing of salen in the solutions which was confirmed by the UV-visible absorbance at 265 and 378 nm. This result means that only some salen could be incorporated in the silica. In addition, the amount of salen that could be doped in the mesoporous silica was found to be quantitative for both temperatures used during the synthesis. However, from the data given in Table 4.2, it could be obviously seen that when the temperature was risen up from 40 °C to 60 ºC, the amount of incorporated salen was significantly increased. It could thus be summarized that the temperature had a profound effect on the preparation of salen doped mesoporous silica. Therefore, further synthesis experiments were performed at 60 ºC.

Table 4.2 Effect of the synthesis temperature on the amount of incorporated salen.

Temperature (°C)	Salen/TEOS (mmole/mole)			Incorporated salen (%)
	use in the synthesis	presence in the solutions	incorporation	
40	3.61	3.10	0.510	14.1
60	3.61	2.27	1.34	37.1

4.2.1.2. Effect of salen quantity on the synthesis of salen doped mesoporous silica.

The amount of salen in the sorbent is a crucial factor that could influence the adsorption properties of the modified silicas. Therefore, in method I, various concentrations of salen were applied for the synthesis. It was found that, in all cases, not the whole amount of the salen added in the synthesis mixture could be encapsulated in the silica. The relation between the quantity of salen used for the synthesis and the amount of incorporated salen was displayed in Table 4.3 and Figure 4.1.

Table 4.3 Effect of salen concentration used for the synthesis on the amount of salen incorporated in the mesoporous silica.

Salen concentration (x 10^{-2} M)	Salen/TEOS (mmole/mole)		Incorporated salen (%)
	use in the synthesis	incorporation	
0.787	5.99	1.39	23.2
1.13	8.62	2.58	29.9
1.82	13.9	3.95	28.3
2.49	19.2	4.85	25.3
3.07	23.4	5.26	22.5

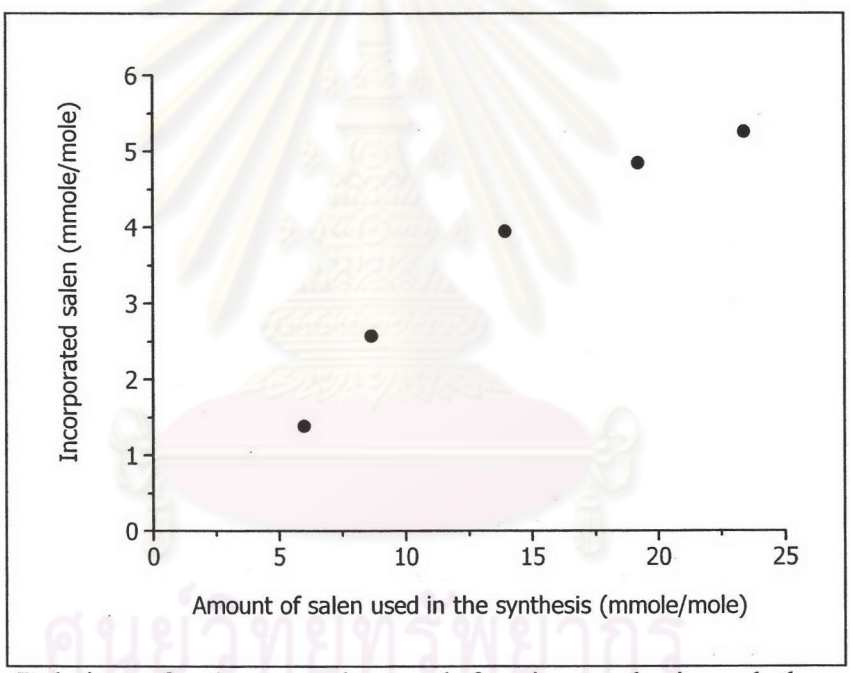

Figure 4.1 Relation of salen quantity used for the synthesis and the amount of incorporated salen.

In combining the results shown in Table 4.3 with that of Figure 4.1, the amount of incorporated salen seemed to be increased with increasing of salen concentration. The maximum amount of incorporated salen was about 30% of the amount of salen used for the synthesis. However, the preparation of salen doped mesoporous silica from higher salen concentration could not be done due to the difficulty in dissolving salen. (In this case, the maximum concentration of salen that could be prepared was 3.07×10^{-2} M). Thus further synthesis procedure was focused on

method II, in which the amount of salen used in the synthesis was also varied. The outcome from this study was demonstrated in Table 4.4 and Figure 4.2. It was lucidly seen that an increase in the amount of salen addition in the synthesis led to an increase in the amount of incorporated salen. And the maximum amount of incorporated salen was obtained when the mole ratio of salen/TEOS used in the synthesis equaled to 120.0 mmole/mole.

Table 4.4 Effect of salen quantity used for the synthesis of salen doped mesoporous silica by method II on the amount of incorporated salen.

Salen/TEOS (mmole/mole)		Incorporated salen (%)	RSD (%)
use in the synthesis	incorporation		
7.69	1.51	19.7	-
13.9	3.03	21.8	6.35[a]
15.2	3.50	23.0	-
23.4	6.48	27.7	8.76[a]
30.2	7.50	24.8	-
30.6	8.30	27.1	-
49.9	12.3	24.7	-
60.0	27.2	45.3	0.780[b]
69.9	40.0	57.2	-
80.0	47.9	59.9	2.40[a]
90.0	62.3	69.2	-
100	63.9	63.9	-
120	90.8	75.7	-

[a] %RSD based on four replicate syntheses.

[b] %RSD based on two replicate syntheses.

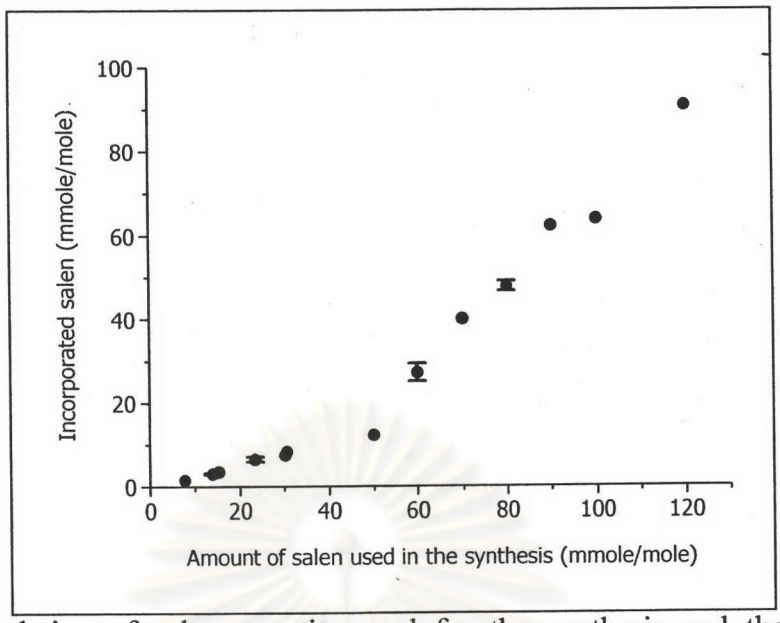

Figure 4.2 Relation of salen quantity used for the synthesis and the amount of incorporated salen of salen doped mesoporous silica synthesized by method II.

Table 4.5 The amount of incorporated salen from different synthesis of salen doped mesoporous silica.

Synthesis number	Incorporated salen/TEOS (mmole/mole)
1	90.8
2	90.7
3	90.9
4	90.7
5	90.6
6	90.6
7	90.4
8	90.4
9	90.6
Average	*90.6*
SD	*0.0156*
RSD (%)	*0.170*

In addition, the reproducibility of the synthesis of salen doped mesoporous silica was also studied. Nine replicate synthesis of salen doped mesoporous silica by Method II were conducted. The results on the amount of incorporated salen were tabulated in Table 4.5. From this table, it could be concluded that the reproducibility of the synthesis was excellent since the standard deviation was only 0.170%. Accordingly, the mole composition used for further synthesis experiments of salen doped mesoporous silica was 1 TEOS : 140 H_2O (0.1 M NaOH) : 0.18 CTAB : 13 EtOH : 0.12 Salen.

4.2.2. Saltn doped mesoporous silica

Two synthesis methods similar to that which described for the synthesis of salen doped mesoporous silica were used to prepare the saltn doped mesoporous silica. And in this time, saltn was used as doping molecules. The amount of loading saltn used for the synthesis was also varied in order to find the maximum amount of incorporated saltn. In Method I, various concentrations of saltn solution were used for the preparation of saltn doped mesoporous silica. From every synthesis result, the obtained modified silicas were orange coloration. The results obtained from the measurement of saltn in the supernatant and washing solutions by UV-visible spectroscopy showed the characteristic spectrum of saltn at 265 nm and 378 nm. This indicated that only some amounts of saltn used for the synthesis could be incorporated into the silica. Table 4.6 showed the relation between the quantity of saltn used for the synthesis and the amount of incorporated saltn.

Table 4.6 Effect of saltn concentration on the amount of incorporated saltn.

Saltn concentration (x 10^{-2} M)	Saltn/TEOS (mmole/mole)		Incorporated saltn (%)
	use in the synthesis	incorporation	
0.334	2.55	0.430	16.9
0.256	2.75	0.610	22.2
3.08	23.6	9.25	39.2
4.05	31.0	9.80	31.6

From Table 4.6, the increasing amount of saltn in the synthesis caused an enhancement of the incorporated saltn in the mesoporous silica. However, the maximum incorporated saltn was limited at 9.80 mmole of saltn per 1 mole of TEOS because of the same difficulty in dissolving the Schiff's base molecules as described previously in section 4.2.1.2. Thus, in order to enhance the quantity of incorporated saltn, various amount of these doping molecules were used to prepare the saltn doped mesoporous silica by Method II. The results on incorporated saltn obtained by the latter method was tabulated in Table 4.7. According to these results, it was immediately obvious that the amount of saltn used in the synthesis had a strongly influence on the amount of incorporated saltn. And the maximum value was obtained when the mole ratio of saltn/TEOS used in the synthesis was equaled to 100 mmole/mole.

Table 4.7 Effect of saltn quantity used for the synthesis of saltn doped mesoporus silica by Method II on the amount of incorporated saltn.

Saltn/TEOS (mmole/mole)		Incorporated saltn (%)
use in the synthesis	incorporation	
30.0	0.558	18.6
60.0	20.4	34.0
100	43.5	43.5

In addition, to determine the reproducibility of the preperation process, the synthesis of saltn doped mesoporous silica was repeated ten times using the mole composition of 1 TEOS : 140 H_2O (0.1 M NaOH) : 0.18 CTAB : 0.1 Saltn. It was found that the average amount of incorporated saltn was 43.5 mmole per 1 mole of TEOS with 2.46 % RSD. Thus, this mole composition was applied for further synthesis of saltn doped mesoporous silica.

4.2.3. Salophen doped mesoporous silica

The synthesis of salophen doped mesoporous silica was conducted as the same manner of the former materials. Again, the amount of salophen used for the synthesis was the main factor for the synthesis of this modified material. In Method I, the concentration of the salophen used for the synthesis was varied between 4.0 mM to 10

mM. Similar conclusions were obtained: only some salophen molecules could be incorporated into the silica and the amount of incorporated salophen increased linearly with the increasing of the amount of salophen used for the synthesis (see Table 4.8 and Figure 4.3). However, the maximum incorporated salophen was limited at 8.12 mmole per 1 mole of TEOS due to the trouble of solubility of Schiff's base ligand as mentioned before. Thus, to increase the maximum amount of incorporated salophen, Method II became a procedure of interest. For the latter method, the synthesis of salophen doped mesoporous silica was performed in duplicated and the mole ratio of salophen/TEOS used for the synthesis equaled to 30, 60, 70 and 80 mmole/mole. The results from all experiments were presented in Table 4.9 and Figure 4.4. It could be seen that the amount of incorporated salophen tended to increase with the increasing of salophen used for the synthesis. The maximum incorporated salophen was obtained when the mole ratio of salophen/TEOS was 80.0 mmole/mole. By using this maximum mole ratio, the preparation of this functionalized silica was repeated seven times to ensure the reproducibility of the synthesis procedure. The series of experiments were carried out and it was found that the average amount of incorporated salophen was 46.0 mmole per 1 mole of TEOS with 1.56% RSD. From the results, the preparation of salophen doped mesoporous silica was also shown an excellent reproducibility procedure. Thus, the mole composition of salophen doped mesoporous silica at 1 TEOS : 140 H_2O (0.1 M NaOH) : 0.18 CTAB : 13 EtOH : 0.08 salophen was used for further experiments.

Table 4.8 Effect of salophen concentration on the amount of incorporated salophen.

Salophen concentration (x 10^{-2} M)	Salophen/TEOS (mmole/mole)		Incorporated salophen (%)
	use in the synthesis	incorporation	
0.483	3.69	0.280	7.59
0.682	5.20	0.690	13.3
0.812	6.20	0.960	15.5
1.06	8.12	1.32	16.3

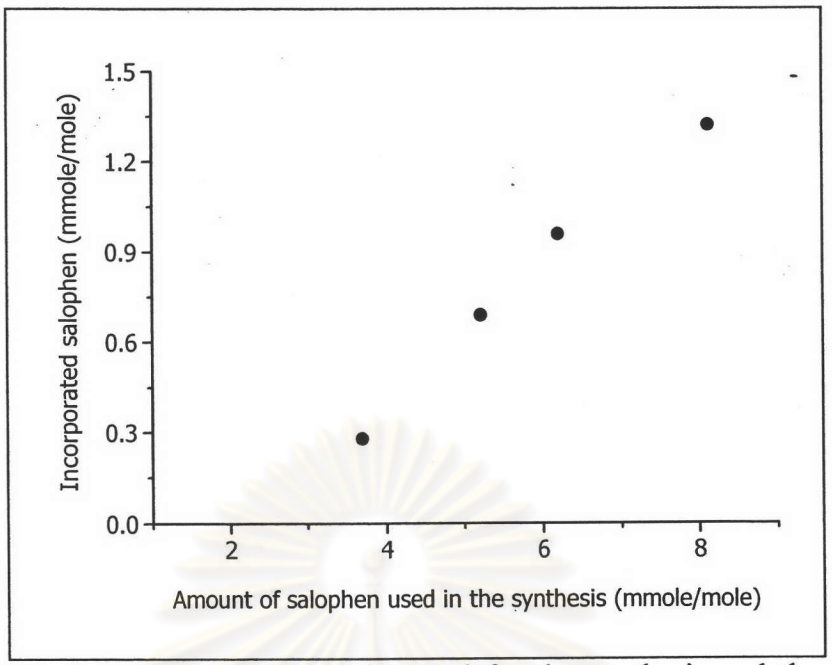

Figure 4.3 Relation of salophen quantity used for the synthesis and the amount of incorporated salophen.

Table 4.9 Effect of salophen quantity used for the synthesis of salophen doped mesoporous silica by Method II on the amount of incorporated salophen.

Salophen/TEOS (mmole/mole)		Incorporated salophen (%)	RSD (%)
use in the synthesis	incorporation		
30.0	9.50	31.7	6.73
60.0	23.3	38.8	3.03
70.0	32.6	46.6	6.52
80.0	46.9	58.6	1.56

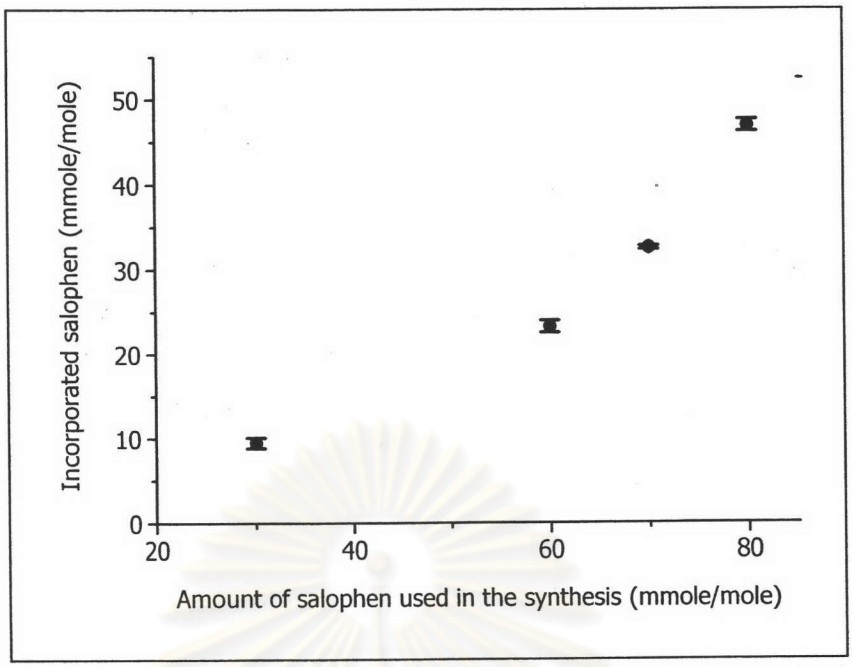

Figure 4.4 Relation of salophen quantity used for the synthesis of salophen doped mesoporous silica by method II and the amount of incorporated salophen.

4.2.4. Haen doped mesoporous silica

From the aforementioned results of the synthesis of the three Schiff's base doped mesoporous materials, it was demonstrated that the limit of the solubility of Schiff's base molecules restricted the amount of incorporated Schiff's base into the mesoporous silica. Therefore, the synthesis of haen doped mesoporous silica was performed according to Method II only. Also, the maximum quantity of incorporated haen was considered by using various amounts of haen for the synthesis. Similar phenomenon during the synthesis was observed. The supernatant and washing solutions were yellow in color due to the presence of haen in the solutions. This cause could be confirmed by the peak of haen at 324 nm in UV-visible spectrum of both solutions. The amounts of incorporated haen in each synthesis were collected in Table 4.10 and the relation between the quantity of haen used for the synthesis and the amount of incorporated haen was displayed in Figure 4.5.

Table 4.10 Effect of haen quantity used for the synthesis of haen doped mesoporous silica by Method II on the amount of incorporated haen.

Haen/TEOS (mmole/mmole)		Incorporated haen (%)	RSD[a] (%)
use in the synthesis	incorporation		
30.0	9.70	32.3	-
60.0	27.0	45.0	3.03
80.0	42.5	53.1	6.52
100	67.0	67.0	-

[a] %RSD based on two replicate syntheses.

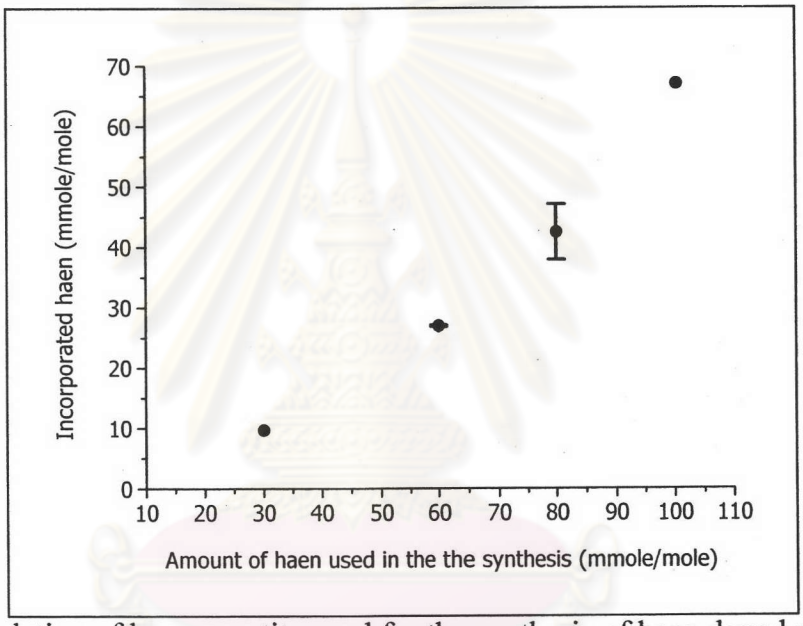

Figure 4.5 Relation of haen quantity used for the synthesis of haen doped mesoporous silica by method II and the amount of incorporated haen.

According to the results from the experiment, it was observed that the increasing amount of haen used in the synthesis could be correlated to the increase in the amount of incorporated haen. The optimum mole ratio of haen/TEOS equaled to 100.0 mmole/mole showed the highest incorporation of haen. For achieving the best modified silica in terms of the reproducibility of the synthesis, eight haen doped mesoporous silica were synthesized using the same composition. And the average of 62.6 mmole of incorporated haen per 1 mole of TEOS was obtained with 0.17% RSD. This value confirmed the excellent reproducibility in the synthesis of haen doped mesoporous silica. Thus, the mole composition used for further synthesis of this material was 1 TEOS : 140 H_2O (0.1 M NaOH) : 0.18 CTAB : 13 EtOH : 0.10 Haen.

4.3. Characterization of materials

4.3.1. Determination of organic matter contents in silica.

The determination of organic matter contents in silica was evaluated by three methods, including calcination, thermogravimetric analysis and elemental analysis. Each method was conducted and then the results from the experiments were illustrated as follows.

4.3.1.1. Calcination

The calcination technique was used to find the amount of organic matters in the as-synthesized silica. The values from the experiment were collected to compare with the calculated data obtained from the mole compositions of each material (theoretical values), which were explained in Appendix B. The results obtained from all mesoporous silica were displayed in Table 4.11 - 4.15.

Table 4.11 Organic matters in non-doped mesoporous silica prepared from different synthesis.

Synthesis number	Organic matters (%)		$\frac{\text{experimental value}}{\text{theoretical value}} \times 100$ (%)
	Experimental value	Theoretical value	
1	46.98	46.12	101.9
2	46.14	46.12	100.0
3	47.48	46.06	103.1
4	46.26	46.05	100.0
5	46.45	46.02	100.9
6	45.35	46.02	98.5
7	46.57	46.02	101.2

Table 4.12 Organic matters in salen doped mesoporous silica synthesized by different methods and contained various amounts of incorporated salen.

Method	Incorporated salen/TEOS (mmole/mole)	Organic matter contents (%)		$\frac{\text{experimental value}}{\text{theoretical value}} \times 100$ (%)
		Experimental value	Theoretical value	
I	1.34	47.75	46.18	103.4
	1.39	47.26	46.20	102.3
	2.58	47.61	46.35	102.7
	3.90	48.11	46.59	103.3
	3.94	47.90	46.53	102.9
	5.33	47.90	46.73	102.5
	4.30	48.95	46.57	105.1
II	1.51	48.57	46.47	104.5
	2.70	47.85	46.38	103.2
	3.20	47.80	46.43	102.9
	8.30	48.10	48.14	99.9
	12.3	52.40	47.68	109.9
	90.6	59.20	55.68	106.3

Table 4.13 Organic matters in saltn doped mesoporous silica synthesized by Method II and contained various amounts of incorporated saltn.

Incorporated saltn/TEOS (mmole/mole)	Organic matter contents (%)		$\frac{\text{experimental value}}{\text{theoretical value}} \times 100$ (%)
	Experimental value	Theoretical value	
0.590	50.30	46.10	109.1
20.4	53.26	48.68	109.4
19.6	55.40	48.28	114.8
43.5	58.43	51.40	113.7

Table 4.14 Organic matters in salophen doped mesoporous silica synthesized by Method II and contained various amounts of incorporated salophen.

Incorporated salophen/TEOS (mmole/mole)	Organic matter contents (%)		$\frac{\text{experimental value}}{\text{theoretical value}} \times 100$ (%)
	Experimental value	Theoretical value	
9.00	50.69	47.36	107.0
23.8	54.51	49.43	110.3
32.7	55.37	50.61	109.4
46.9	58.35	52.35	111.4

Table 4.15 Organic matters in haen doped mesoporous silica synthesized by Method II and contained various amounts of incorporated haen.

Incoporated haen/TEOS (mmole/mole)	Organic matter contents (%)		$\frac{\text{experimental value}}{\text{theoretical value}} \times 100$ (%)
	Experimental value	Theoretical value	
9.70	50.15	47.52	105.5
27.1	54.24	49.83	108.8
39.2	56.70	51.43	110.2
62.6	58.32	54.17	107.7

As could be seen from all tables that the amounts of organic matters obtained from the experiment in all mesoporous silica were slightly higher than the theoretical values. The minor difference might be explained by the amounts of physisorbed water and chemisorbed water, which were still in the framework of silica before the beginning of calcination experiment. In fact, the physisorbed and chemisorbed water could be eliminated at about 170 °C and 400 °C, respectively [6].

4.3.1.2. Thermogravimetric analysis

Thermogravimetric method is also available for the determination of the amount of organic matters in silica. This technique provides informations about the weight loss steps corresponding to physically adsorbed water, organic and surfactant molecules thermodesorption, and silanol condensation. In this thesis, the modified mesoporous silica, which had the maximum amount of incorporated Schiff's base

molecules were brought to study. The TGA and DTG curves of all as-synthesized mesoporous silica were exhibited in Figure 4.6 - 4.10. The percentages of weight loss obtained from TGA curves for all materials were also summarized in Table 4.16.

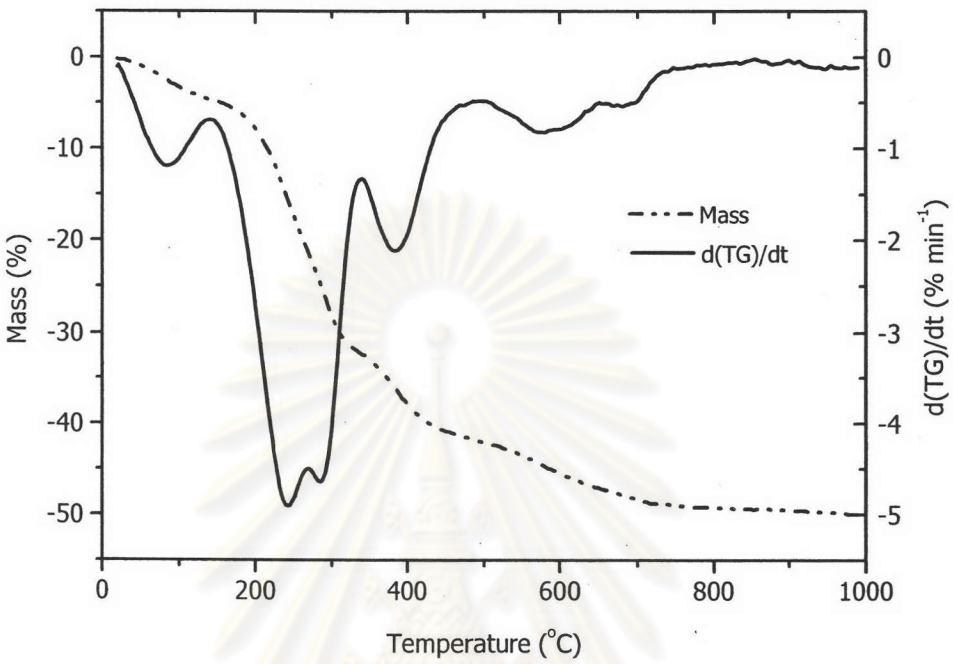

Figure 4.6 TGA and DTG curves of non-doped mesoporous silica.

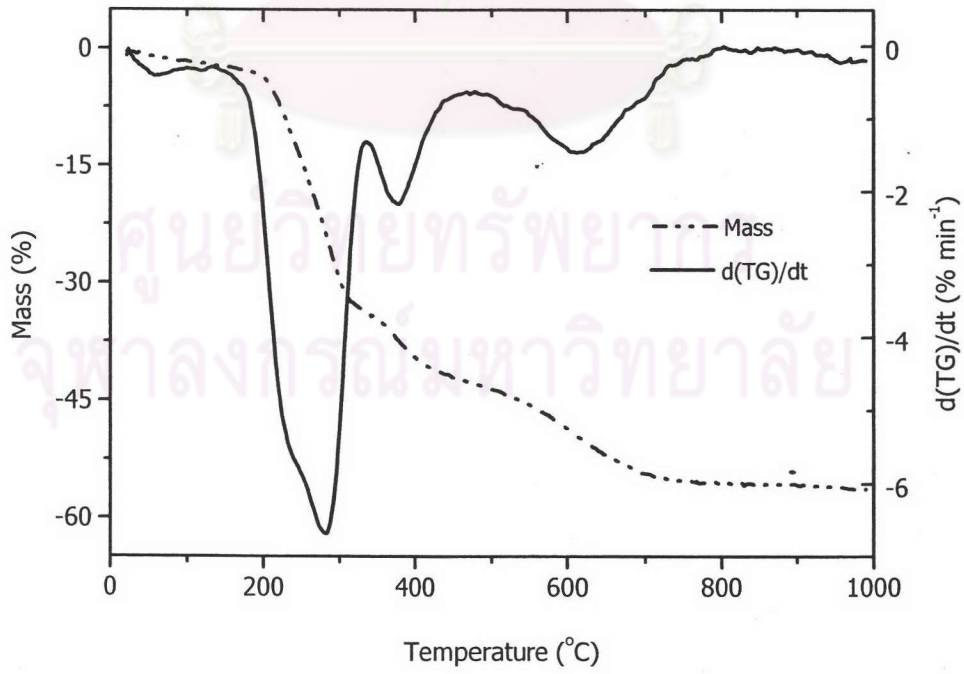

Figure 4.7 TGA and DTG curves of salen doped mesoporous silica.

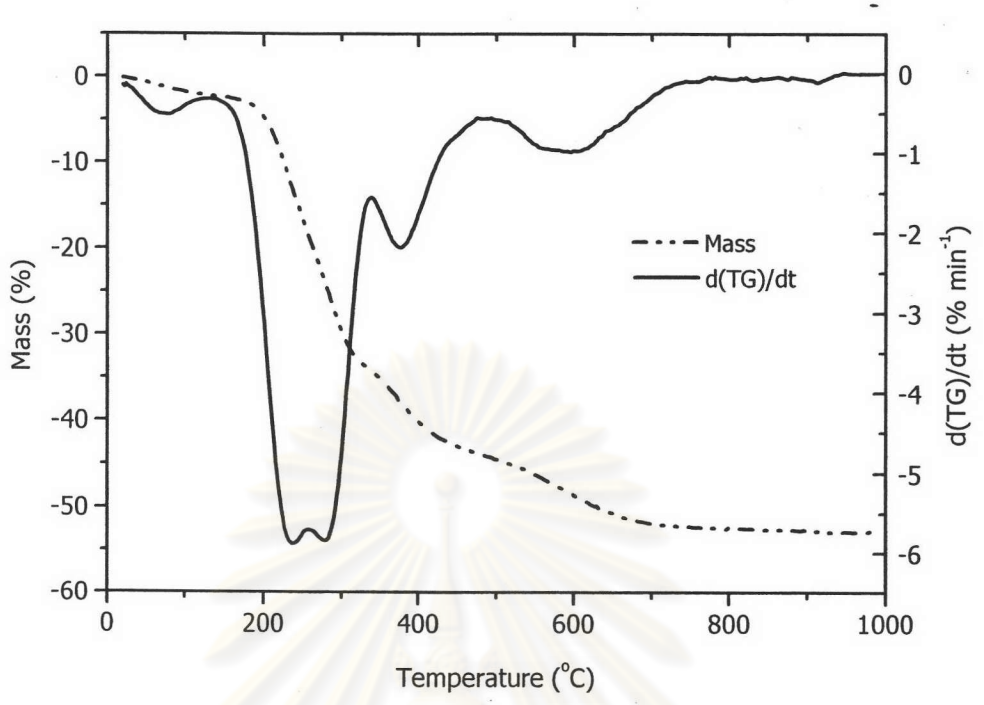

Figure 4.8 TGA and DTG curves of saltn doped mesoporous silica.

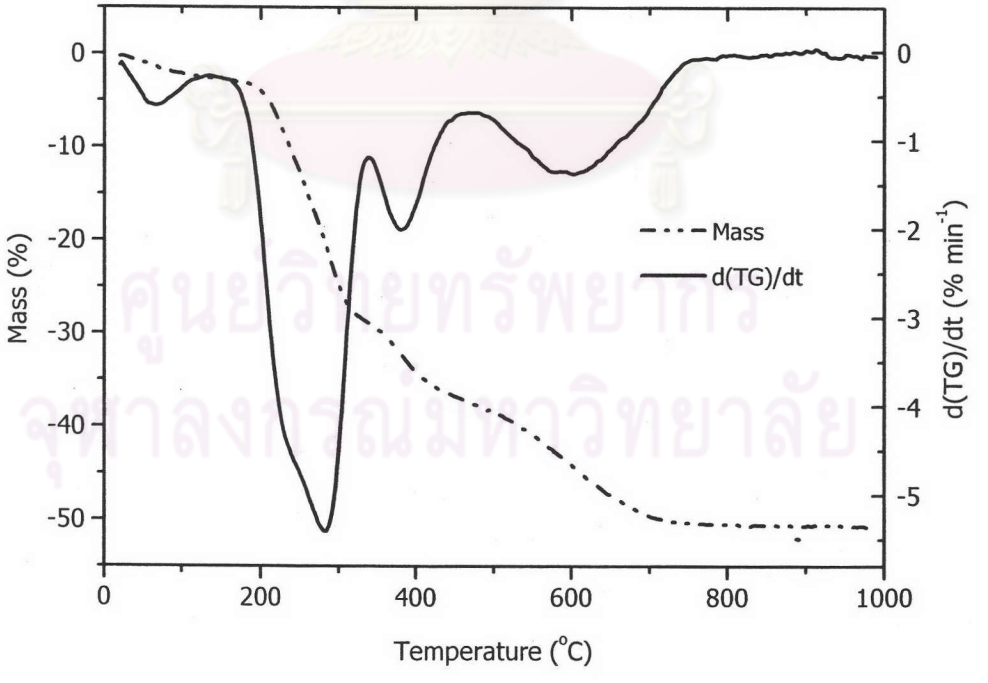

Figure 4.9 TGA and DTG curves of salophen doped mesoporous silica.

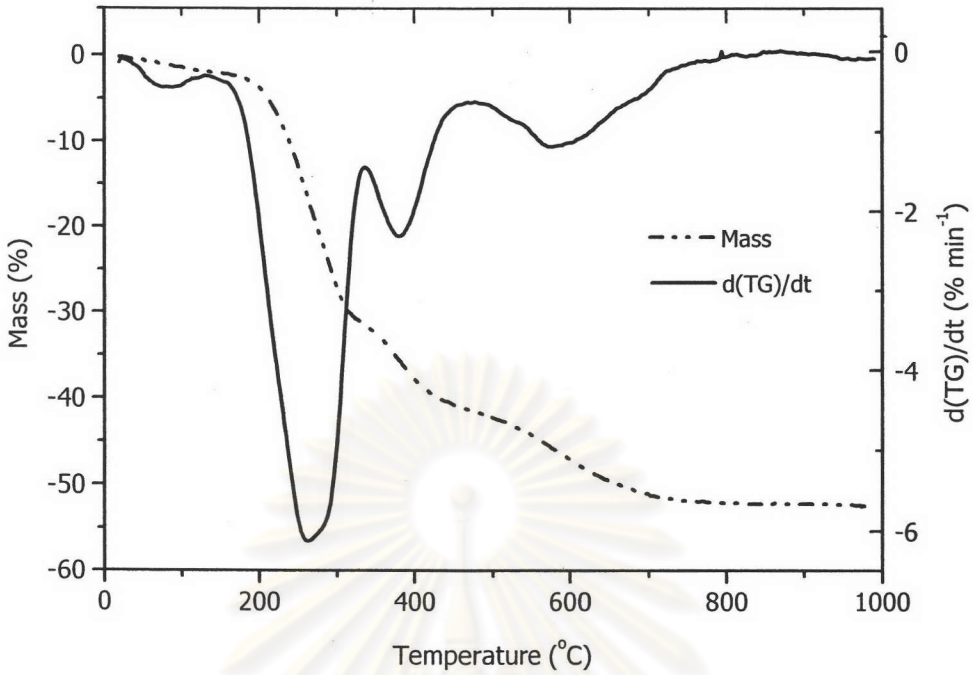

Figure 4.10 TGA and DTG curves of haen doped mesoporous silica.

Table 4.16 The weight loss from TGA results of the as-synthesized mesoporous silica.

Type of silica	Weight loss (%) at different temperature regions (°C)				Total weight loss (%)
	20-150	150-330	330-500	500-700	
Non-doped	4.90	27.2	10.0	7.90	50.0
Salen doped	2.30	32.0	9.40	12.8	56.2
Saltn doped	2.20	32.8	10.3	8.40	52.9
Salophen doped	2.70	26.0	8.80	13.2	50.7
Haen doped	2.50	29.0	10.1	10.2	52.5

As could be seen from these figures, all TGA curves showed analogous behavior. The first mass loss between 20 °C and 150 °C was attributed to the loss of water present in silica. All materials showed a further mass loss started at 150 °C and was completely removed at 700 °C which was due to desorption and decomposition of both template and doping molecules. In addition, the net weight loss results were in accordance with the theoretical values of organic matter contents displayed in section 4.3.1.1.

4.3.1.3. Elemental analysis

Further evidence of the presence of organic matters in modified silica was demonstrated by elemental analysis. This technique provided the data on the basis of C, H, N analysis. The elemental mass of both non-doped and all four Schiff's base doped mesoporous silica from three replicated experiments and that calculated from the composition of starting materials as shown in Appendix C were collected in Table 4.17.

Table 4.17 Elemental analysis results of the modified mesoporous silica.

Modified silica	Elemental mass (%)					
	C		H		N	
	Theoretical values	Experimental values	Theoretical values	Experimental values	Theoretical values	Experimental values
Non-doped	36.90	33.34±0.05	6.791	6.702±0.202	2.264	1.927±0.021
Salen doped	43.12	39.25±0.29	6.645	5.585±0.208	3.727	3.189±0.224
Saltn doped	40.44	36.36±0.13	6.749	6.000±0.246	3.025	2.570±0.187
Salophen doped	41.48	36.19±0.09	6.587	6.146±0.053	3.038	2.533±0.148
Haen doped	42.36	36.56±0.23	6.787	6.235±0.028	3.351	2.453±0.124

From Table 4.17, the slightly decrease in mass of C, H, N was found for the experimental values in comparison with that of theoretical values. The minor difference was probably due to the loss of some surfactant during the synthesis procedure.

4.3.2. Investigation of organic molecules in mesoporous silica using FT-IR technique.

FT-IR spectroscopic studies presented a useful tool to initially detect the success of the modified solid process [27, 55, 56]. In order to confirm the presence of surfactant and Schiff's base molecules in the modified silica, the synthesized mesoporous silica was then examined by FT-IR spectroscopy. The resulting spectra for non-doped mesoporous silica, salen doped mesoporous silica, saltn doped mesoporous silica, salophen doped mesoporous silica and haen doped mesoporous silica were exhibited in Figures 4.11– 4.15, respectively.

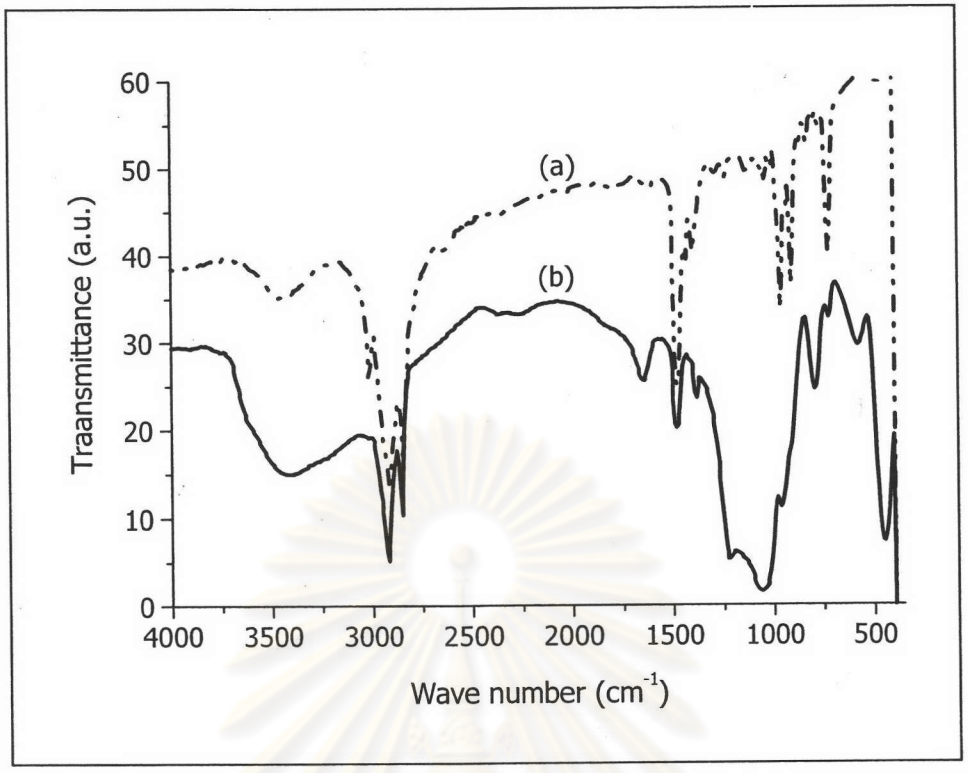

Figure 4.11 FT-IR spectra of (a) CTAB; (b) non-doped mesoporous silica.

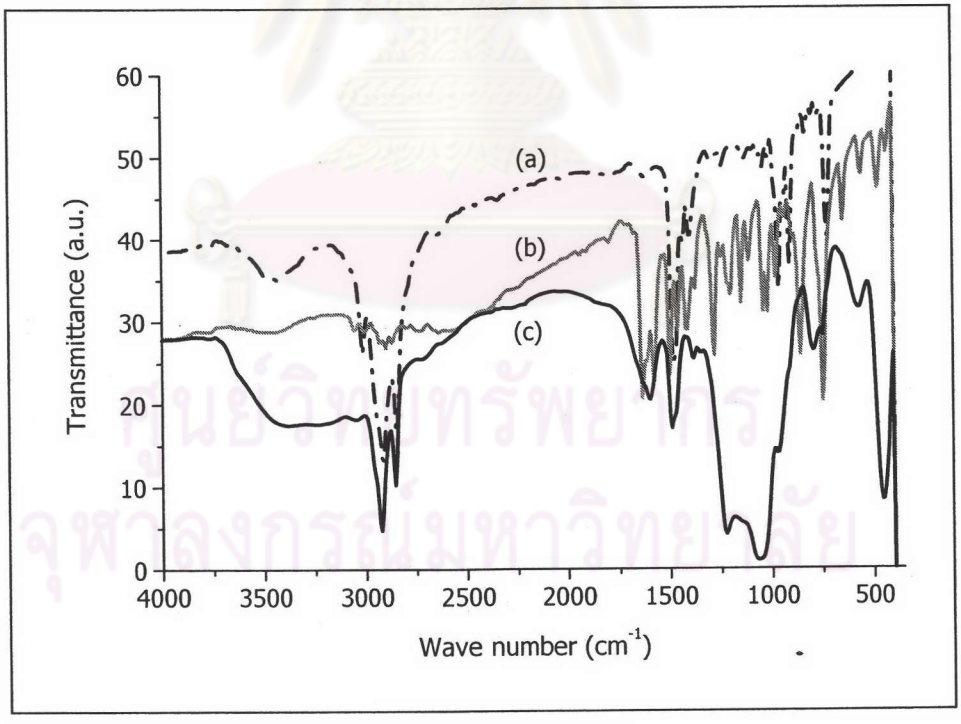

Figure 4.12 FT-IR spectra of (a) CTAB; (b) salen and (c) salen doped mesoporous silica.

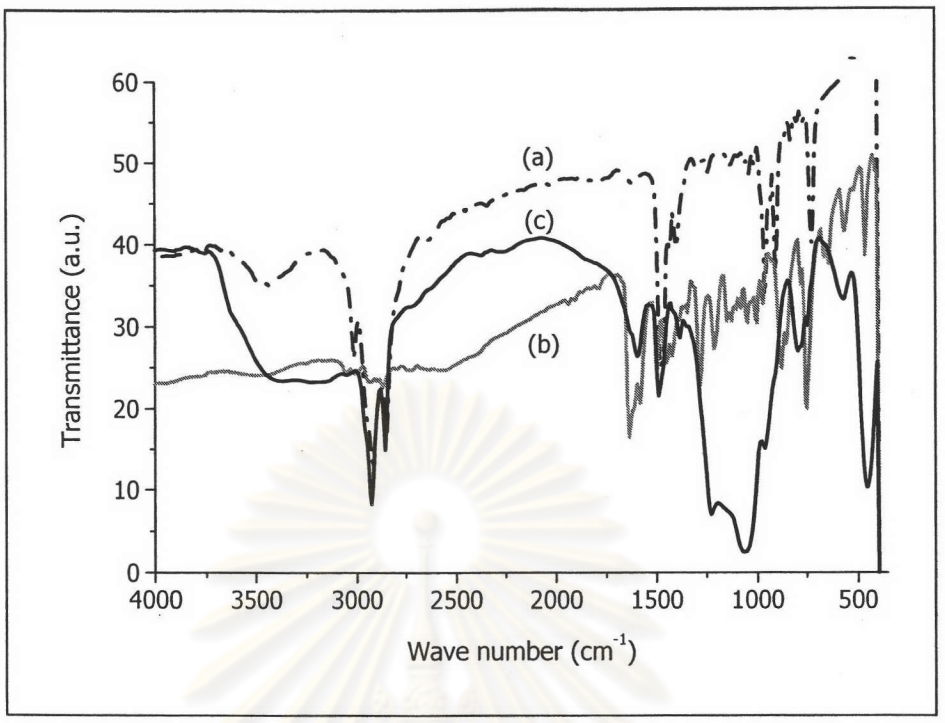

Figure 4.13 FT-IR spectra of (a) CTAB; (b) saltn and (c) saltn doped mesoporous silica.

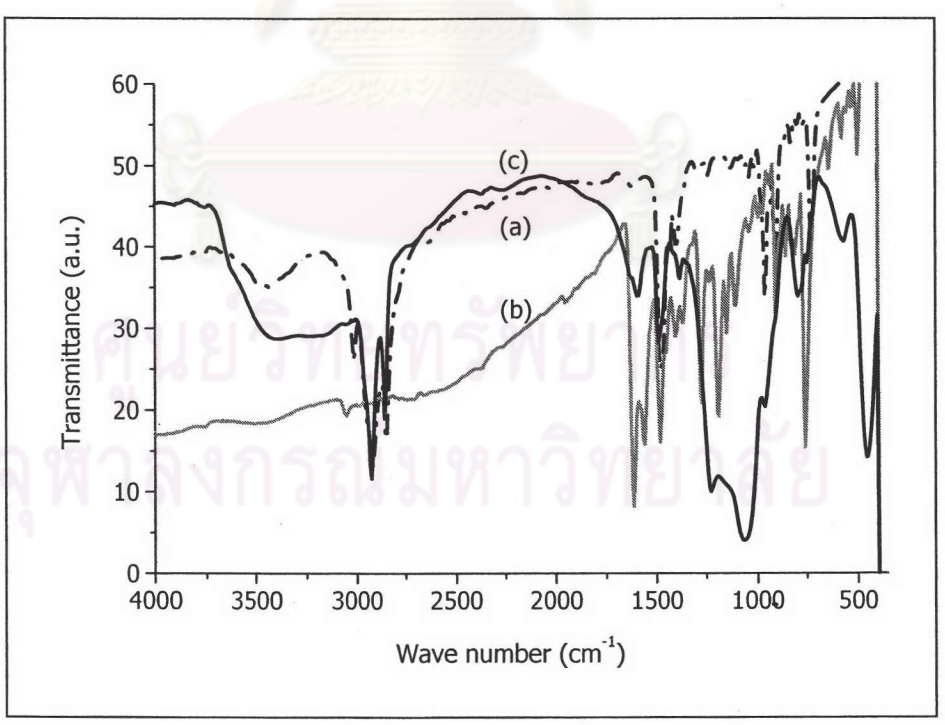

Figure 4.14 FT-IR spectra of (a) CTAB; (b) salophen and (c) salophen doped mesoporous silica.

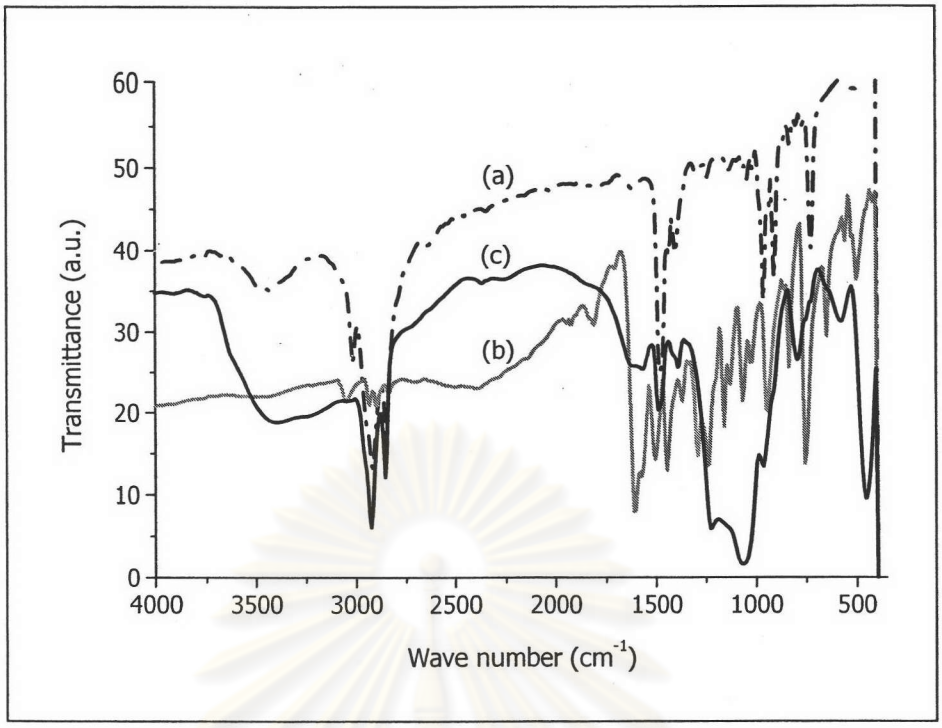

Figure 4.15 FT-IR spectra of (a) CTAB; (b) haen and (c) haen doped mesoporous silica.

As shown in Figure 4.11 (b), the FT-IR spectra of the non-doped mesoporous silica showed the characteristic bands of the silica framework [57]. The peak at 1064 and 794 cm^{-1} correspond to the vibration of the asymmetric and symmetric stretching of Si-O modes, respectively. The band at 440 cm^{-1} was ascribed to the vibration of Si-O-Si bending modes. The Si-OH band appeared at 973 cm^{-1} and very broad absorption band of SiO-H stretching was near 3500 cm^{-1}. The band at 1620 cm^{-1} was assigned to a deformation mode of adsorbed molecular water (O-H stretching). In addition, the spectra in figure 4.11 (b), showed the characteristic bands of CTAB at 2923, 2854 and 1481.5 cm^{-1} for CH stretching.

For FT-IR spectra of salen doped mesoporous silica, the characteristic bands of the silica framework and CTAB were observed at the same position found in FT-IR spectra of non-doped mesoporous silica. Furthermore, this spectrum had also a sharp peak at 1596 cm^{-1} which was the characteristic of the $\nu_{C=N}$ bond, as observed in the spectrum of Figure 4.12 (b). The characteristic $\nu_{C=N}$ bond in the spectrum of salen doped mesoporous silica was evidence of the presence of salen (C=N group) in the structure of the modified silica [41, 58].

The characteristic spectra of other Schiff's base ligands and Schiff's base doped mesoporous silica was similarly demonstrated in Figures 4.13 – 4.15. Considering the FT-IR spectrum of all Schiff's base doped mesoporous silica, all characteristic bands of silica were observed as described previously. These spectra also had two sharp peaks at 2850 and 2925 cm^{-1} that were assigned to the stretching mode of CH_2 groups in CTAB. In addition, the incorporated Schiff's base ligands could be characterized by the presence of a band at about 1600 cm^{-1} corresponding to $\nu_{C=N}$ of the Schiff's base molecules. These IR results confirmed the existence of incorporated Schiff's bases in the related Schiff's base doped mesoporous silica.

4.3.3. Determination of accessible Schiff's bases.

As solvents played an important role in the determination of accessible Schiff's bases, thus, to obtain the maximum accessible Schiff's bases, the effect of solvent were brought to studies. In this work, salen doped mesoporous silica was selected as sample material. And deionized water, acetonitrile (ACN) and ethanol (EtOH) were used as accessible reagents.

The experiments were first performed using solvent mixture of ACN/H_2O or EtOH/H_2O with many variables in volume ratio (*i.e.* 10 : 0, 9 : 1, 1 : 1 and 1 : 9) to extract salen molecules out of silica. The amounts of extracted salen were then determined by UV-visible spectroscopy. The experimental results showed that all solvent mixtures of ACN/H_2O could not extract any salen. On the contrary, when EtOH/H_2O was used, the accessible salen could be determined. Furthermore, among four volume ratios of EtOH/H_2O used, the ratio of EtOH/H_2O equaled to 9 : 1 provided the highest amount of accessible salen. Therefore the solvent mixture of EtOH/H_2O at this volume ratio was used for further determination of accessible Schiff's base ligand in corresponding Schiff's base doped mesoporous silica. The obtained results revealed that salen is the only Schiff's base which could be quantitatively extracted from mesoporous silica, while saltn, salophen and haen could not be extracted in this condition. This phenomenon may be explained by the inappropriate solvent for the three latter ligands or by the inaccessible of these ligands to the solvent.

Further determination of accessible salen was performed on other salen doped mesoporous silica containing different amounts of incorporated salen. The results were exhibited in Figure 4.16. As seen from this figure, the amount of accessible salen was related to those of incorporated salen. However, the maximum amount of accessible salen that could be obtained was only 40% of the total amounts of incorporated salen. This limitation might be caused by the presence of some salen molecules in close pores of silica.

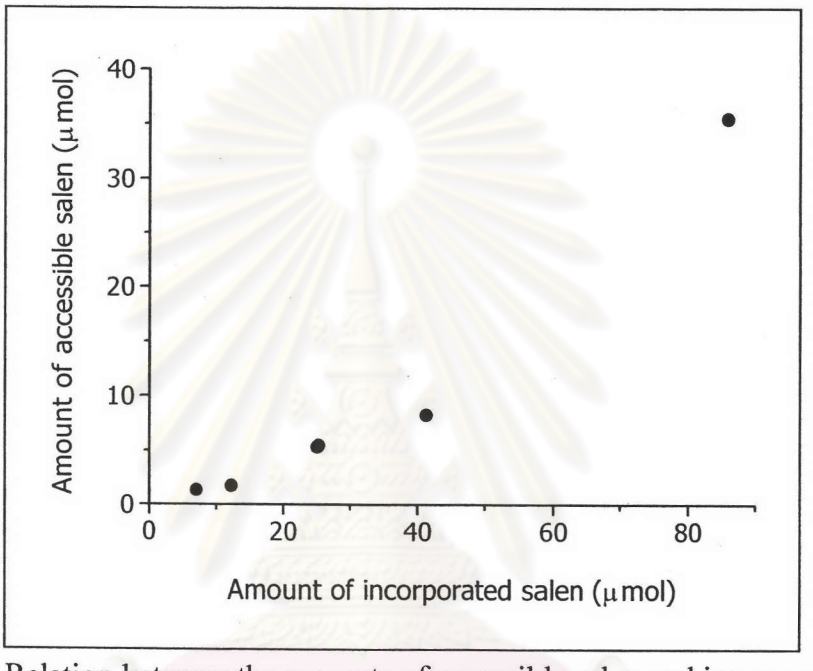

Figure 4.16 Relation between the amounts of accessible salen and incorporated salen.

4.3.4. Crystallinity and morphology of modified mesoporous silica

4.3.4.1. Crystallinity of materials

In general, intensity, broadness and position of a peak in the XRD patterns indicate the crystallinity of materials. Thus, to confirm the crystallinity of the synthesized mesoporous silica, the solid samples were analyzed using X-ray diffraction technique. The diffractogram of the materials studied were shown in Figure 4.17.

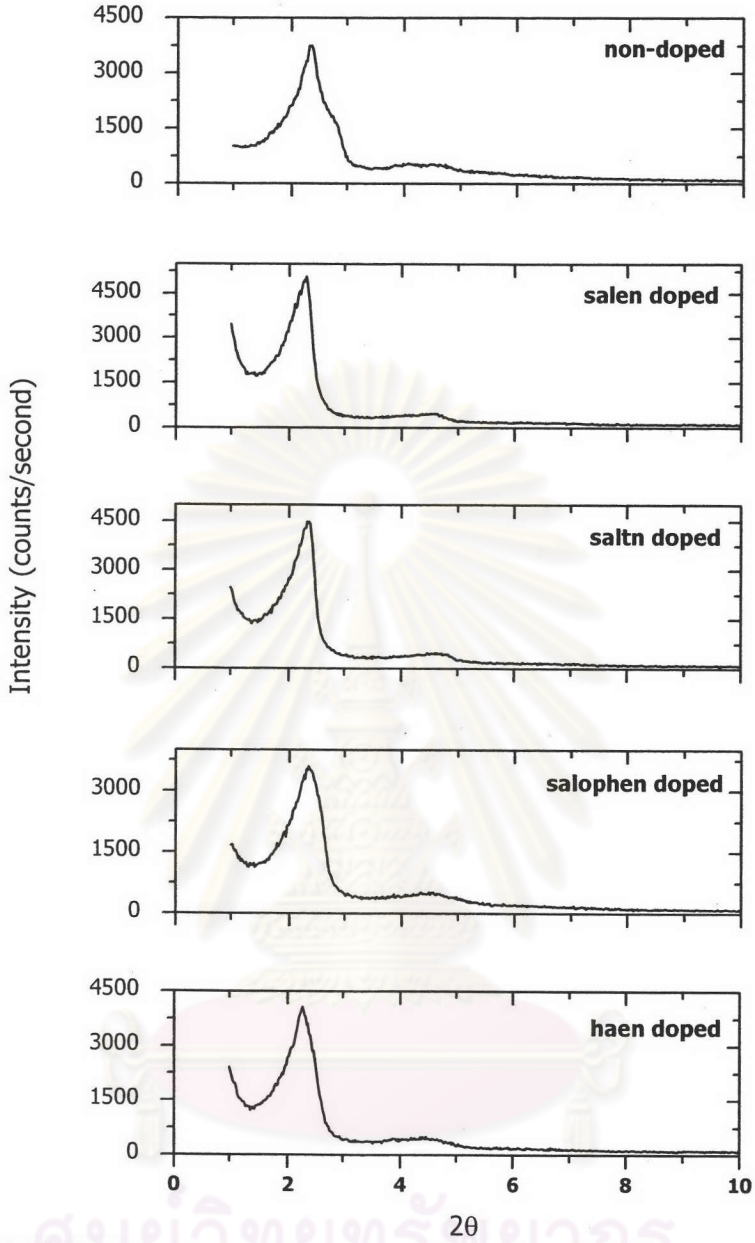

Figure 4.17 XRD patterns of the as-synthesized modified mesoporous silica.

The XRD patterns of the as-synthesized modified mesoporous silica presented the diffraction peaks, which exhibited the crystalline solid structure. Also, all samples showed a very strong peak attributed to (100) reflection around $2\theta \leq 2°$, indicating the presence of periodic mesostructure [59]. Furthermore, the patterns in Figure 4.17 appeared to described a lamellar phase mesostructure, exhibiting strong d_{100} and weak d_{200} reflections. In addition, the XRD patterns of the as-synthesized materials and the corresponding samples measured after the removal of organic template from the pores of mesoporous silica by calcinations at 540 °C were displayed in Figure 4.18. Also,

the d-spacing values of the as-synthesized and the calcined mesoporous silica were summarized in Table 4.18.

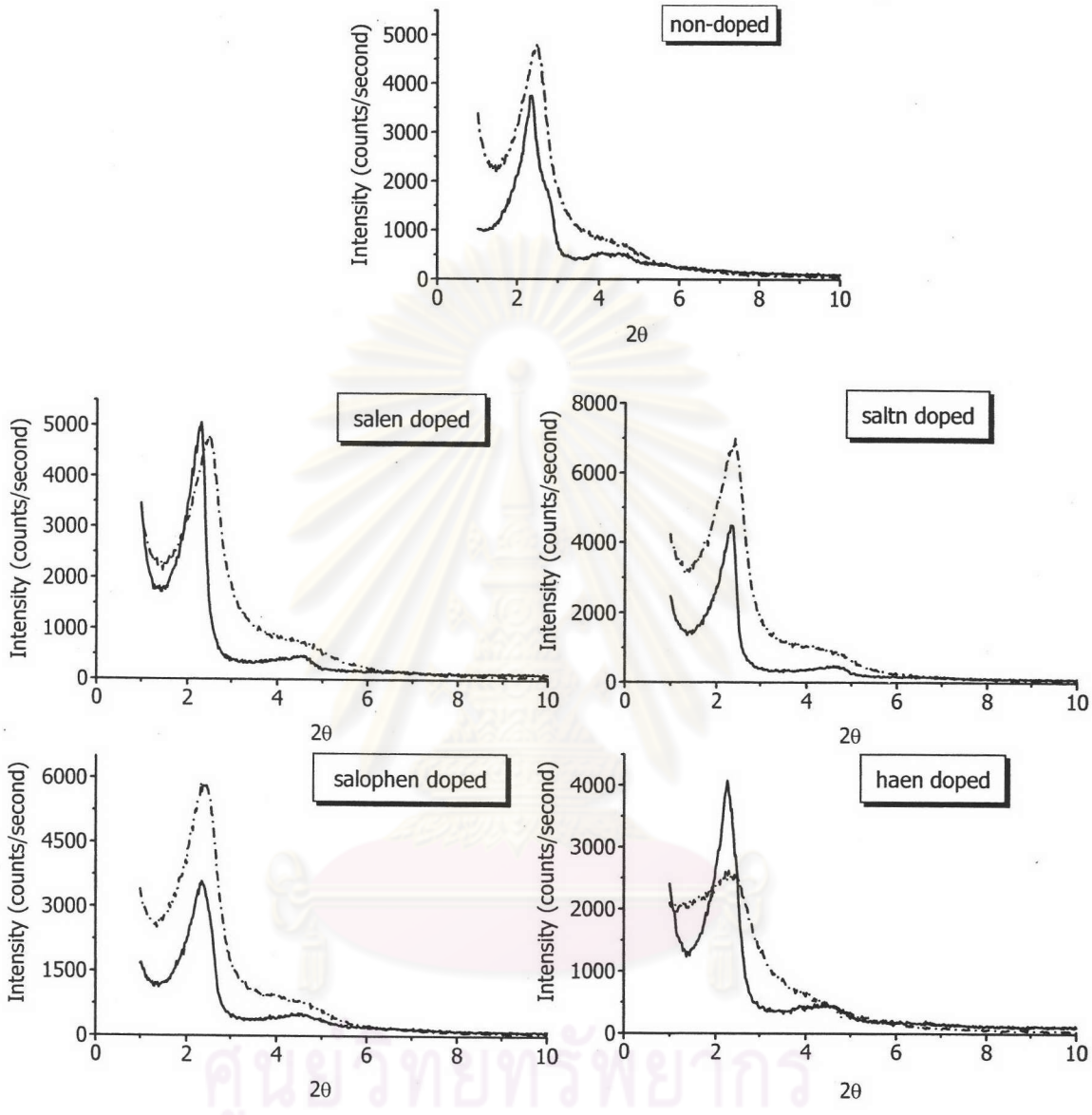

Figure 4.18 X-ray diffraction patterns of the modified silica (solid: as-synthesized silica, dash: calcined silica.)

Table 4.18 XRD data of the as-synthesized and calcined mesoporous silica.

Type of mesoporous silica	As-synthesized silica		Calcined silica	
	2θ	d-spacing (Å)	2θ	d-spacing (Å)
Non-doped	2.30 3.96 4.62	38.38 22.27 19.12	2.48 4.81	35.59 18.38
Salen doped	2.30 4.58	38.39 19.28	2.46 4.59	35.89 19.20
Saltn doped	2.32 4.72	38.04 18.71	2.42 4.73	36.48 18.67
Salophen doped	2.34 4.48	37.72 19.70	2.44 4.36	36.18 20.25
Haen doped	2.26 4.56	39.06 19.36	2.48	35.6

The results from Figure 4.18 and Table 4.18 revealed that the organic template affected the intensity of the reflection peak especially the parent one, in XRD patterns. Apart from haen doped mesoporous silica, in the absence of the template, the intensity of (100) diffraction of all mesoporous silica was slightly increased while a basal peak position was shifted to a higher diffraction angle. The increase in scattering intensity observed here might be due to better ordering of the inorganic framework or increase in scattering domain size. These indicated that the structural ordering was retained in the calcined forms of these silica [60]. Also, the calcination lead to a slight shrinkage in pore size. This was probably due to the condensation of Si-OH groups and the loss of organic molecules during the calcination process [61]. In case of haen doped mesoporous silica, the main XRD line was decreased and higher order lines disappeared. This might be due to a significant degradation of a solid and some collapse, which suggested that the template of this material was unstable towards calcination.

4.3.4.2. Mesoporosity, surface area and pore size

Nitrogen sorption measurement was the most widely used method for the determination of surface area and porous texture of various materials. In order to characterize the texture morphologies of the synthesized mesoporous silica, this technique was used in this study. The functionalized materials were characterized by the determination of their specific surface area through the BET method. The pore size distributions were analyzed following the BJH model. The pore volume calculated from the desorption volume at $P/P_o = 0.99$. The nitrogen sorption isotherms and pore size distributions of the various prepared silica were shown in Figure 4.19 and Figure 4.20, respectively.

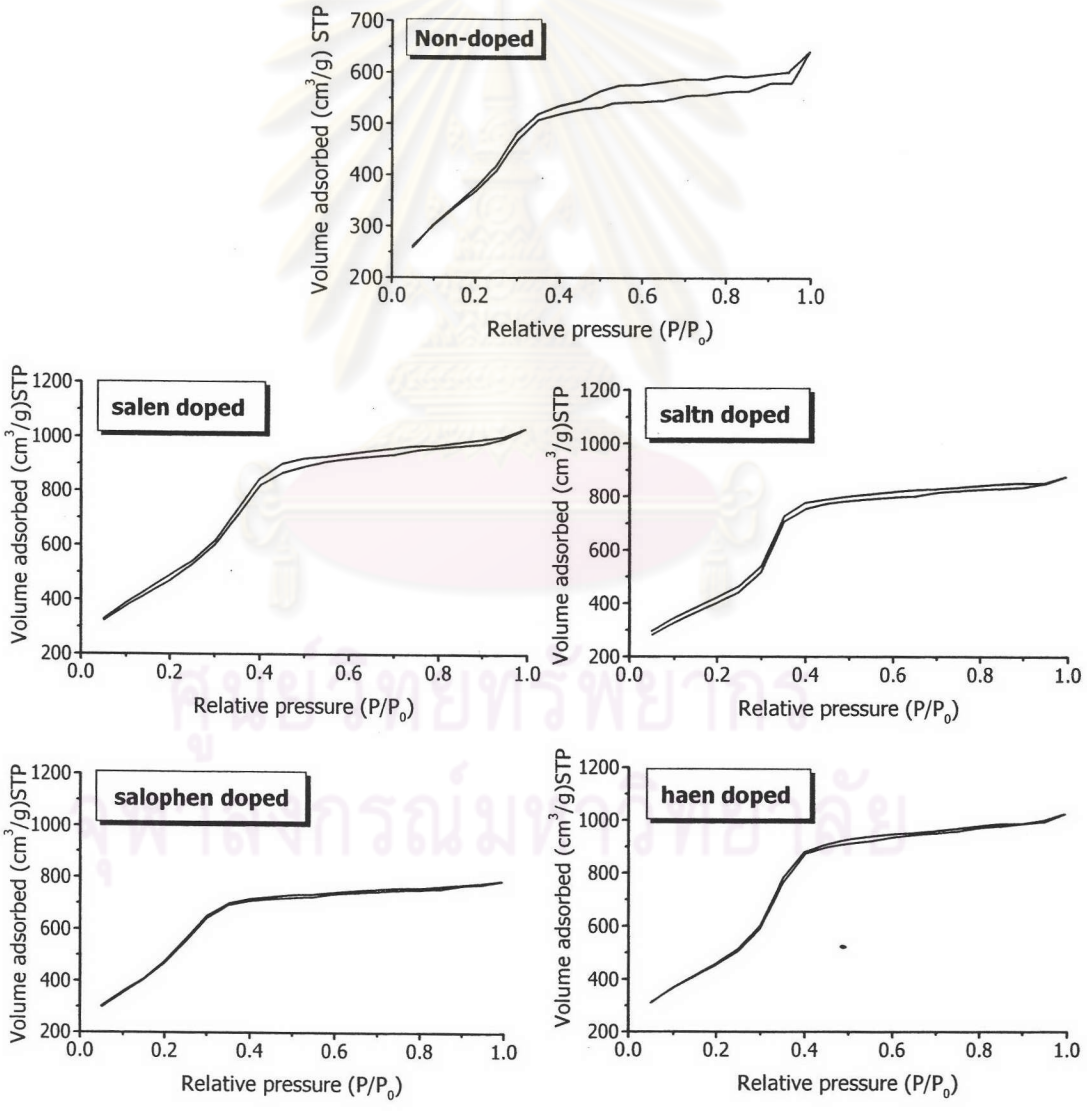

Figure 4.19 Nitrogen sorption isotherms of the modified mesoporous silica.

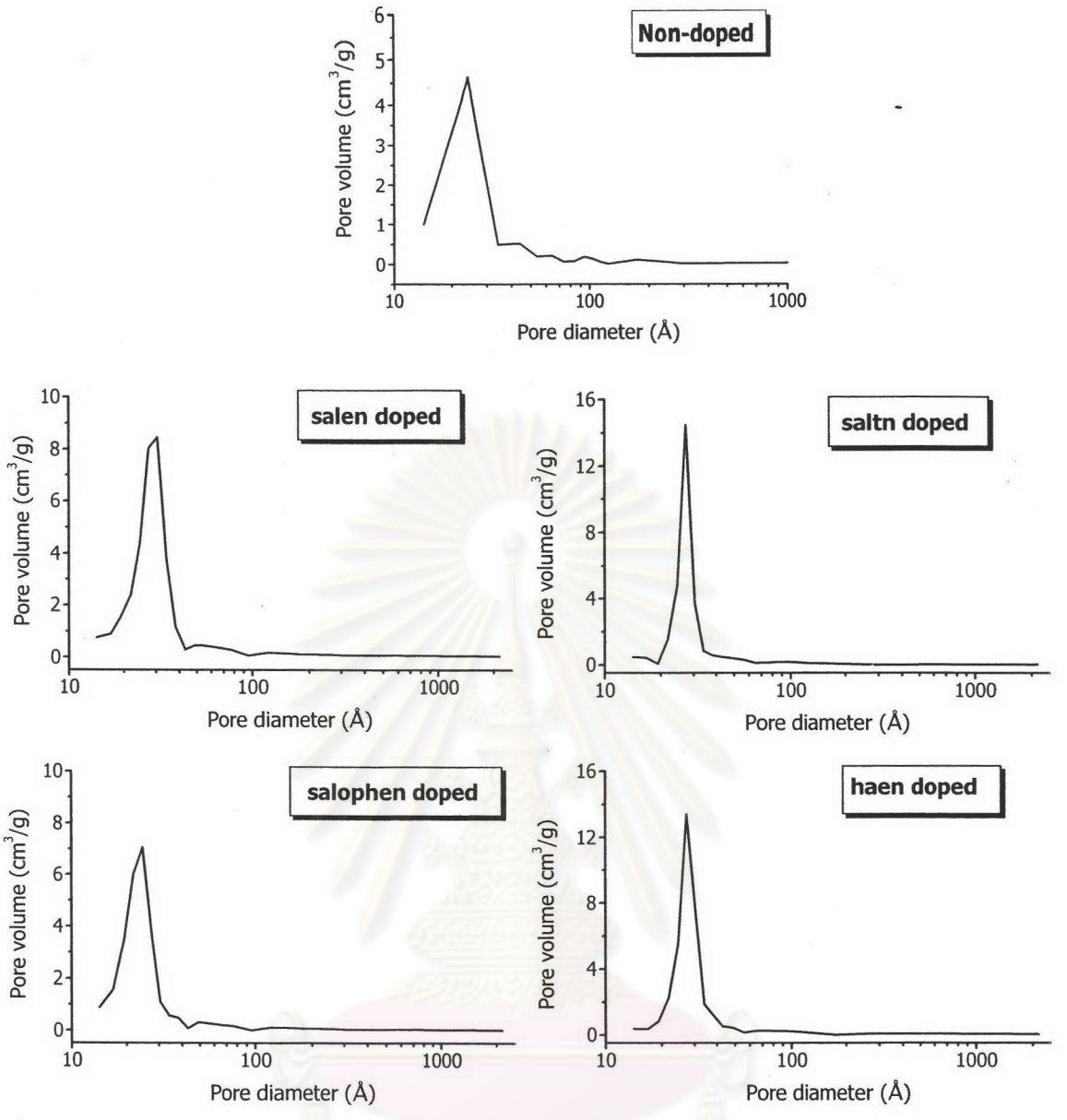

Figure 4.20 BJH pore diameters of the modified mesoporous silica.

The results in Figure 4.19 showed N_2 sorption isotherms at various relative pressure (P/P_o = 0 to 1). Similar phenomena were observed in all samples. A linear increase of absorbed volume at low pressures was followed by a steep increase in nitrogen uptake at a relative pressure of $0.2 < P/P_0 < 0.4$, which was due to capillary condensation inside the mesopore. Thus, all isotherms exhibited the same type IV isotherms with H4 hysteresis loop according to IUPAC, which was the characteristic of mesoporous material with slit-shaped pores [28]. The BJH desorption results from Figure 4.20 confirmed the mesopore of the modified silica with a narrow pore size distribution and a mean value of 24-27 Å. In addition, the BET surface area, pore

volume and mesoporosity were calculated using the isotherms and listed in Table 4.19.

Table 4.19 Textural morphologies of the modified silica determined from N_2 sorption experiments at 77 K and XRD measurements.

Type of silica	d_{100} (Å)	a_0 (Å)	S (m^2/g)	V_p (cm^3/g)	*APD* (Å)	*W* (Å)	*t* (Å)
Non-doped	35.6	41.1	1380	0.99	28.7	24.5	16.6
Salen doped	35.9	41.5	1807	1.60	35.4	27.4	14.1
Saltn doped	36.5	42.1	1504	1.36	36.1	27.4	14.7
Salophen doped	36.2	41.8	1650	1.22	29.6	24.5	17.3
Haen doped	35.6	41.1	1734	1.59	36.7	27.4	13.7

d_{100}, d-value 100 reflections; a_0 = The lattice parameter, from the XRD data using the formula $a_0 = 2d_{100}/\sqrt{3}$; *S*, BET surface area (m^2/g) obtained from N_2 sorption; V_p, Total pore volume (cm^3/g) obtained from single-point volume at $P/P_o = 0.99$; *APD*, average pore diameter calculated from $4V_p/S$; *W*, pore size (Å) obtained from BJH method (The method proposed by Kruk *et. al.* [62]); *t*, pore wall thickness was equaled to $a_0 - W$.

As could be seen from Table 4.19 that all functionalized silica showed the large surface area (1,500-1,800 m^2/g). These values were also higher than the surface area of the mesoporous silica prepared without the incorporation of Schiff's base molecules. This greater values were probably caused by the fact that the regions between the organic groups were spacious enough to accommodate nitrogen molecules when Schiff's base molecules were incorporated into the pore surface of silica. In addition, the pore volume of the non-doped mesoporous silica was much lower than that of the modified silica. These results suggested that the incorporation of Schiff's base molecules by a doping technique brought an extendibility of the pore size and a decrease of the void fraction. Furthermore, the wall thickness values obtained by subtracing the average pore diameter (*APD)* from the lattice parameter (a_0) did not significantly change in any materials. However, the wall thickness of haen doped mesoporous silica at 13.7 Å was lower than those of the other four modified silica which had walls of thickness in the range 14.1 to 17.3 Å. The thinner wall for the haen doped mesoporous silica was consistent with structural collapse during calcination. The textural data of the haen doped mesoporous silica was indicative of lower structural ordering material which was in agreement with the XRD results described earlier.

4.3.4.3. Particle size

The particle size of material was one of the most important physico-chemical parameters for silica [22]. Generally, silica packing can be defined as the average particle diameter distribution. In this thesis, the particle size of all as-synthesized silica was determined by the Malvern laser diffraction technique, which was widely used method. The representative particle size curves of the modified silica based on volume was exhibited in Figure 4.21 and the frequently found particle size of each materials was summarized in Table 4.20.

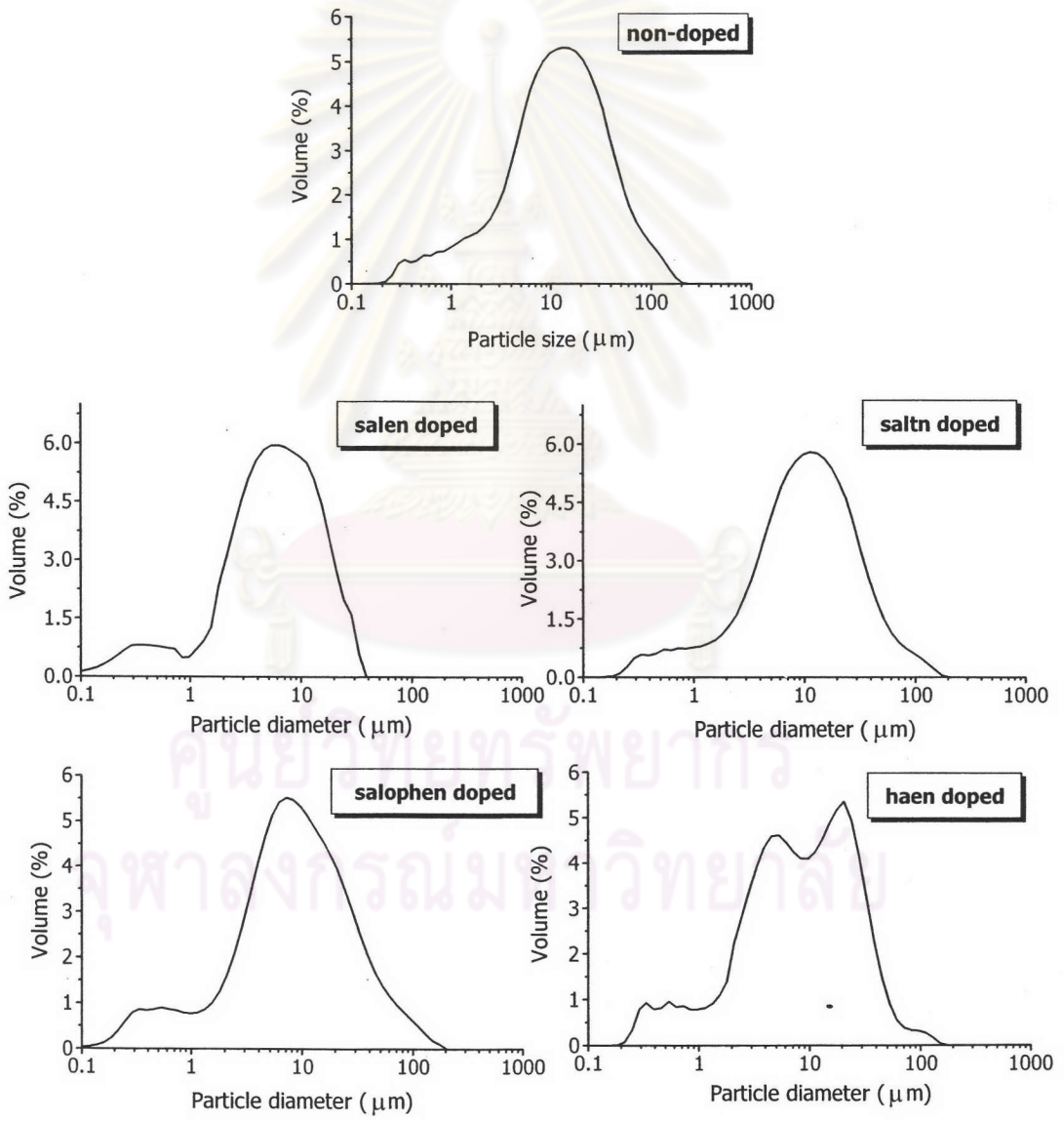

Figure 4.21 Particle diameters of as-synthesized non-doped and Schiff's base doped mesoporous silica.

Table 4.20 The frequently found particle size of as-synthesized mesoporous silica.

Type of silica	Particle size (μm)
Non-doped	11.84
Salen doped	8.640
Saltn doped	10.48
Salophen doped	8.170
Haen doped	9.480 and 23.20

The above experimental results so far clearly indicated that all the modified mesoporous silica had a narrow particle size distribution. The particle size of each modified silica prepared was not significantly different, and all materials had a mean particle size around 8-12 μm.

4.3.4.4. Morphology of materials

The morphology of the as-synthesized silica was determined using scanning electron microscopy (SEM) techniques. The results were displayed in Figure 4.22. The SEM micrograph of the surface of all materials in this figure showed a regular morphology of spherical particles. Among all materials examined, the particle size of salen doped mesoporous silica looked bigger than those respective materials. Considering the mean particle size of salen doped mesoporous silica was about 1.60 μm, whereas the particle sizes of other materials were found to be in the range of 0.40 -0.50 μm.

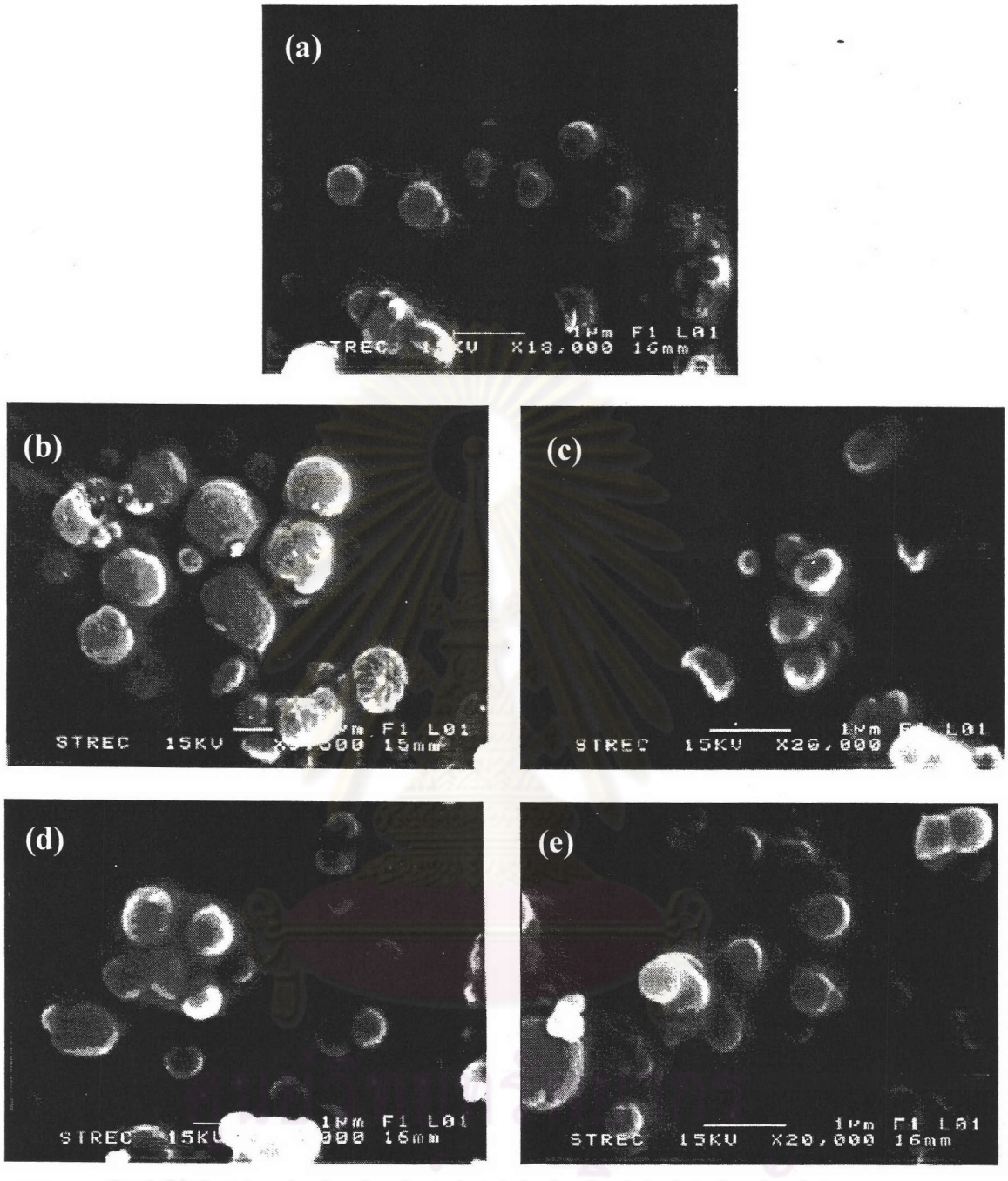

Figure 4.22 SEM images of as-synthesized (a) non-doped, (b) salen doped, (c) saltn doped, (d) salophen doped and (e) haen doped mesoporous silica.

4.4. Extraction properties of materials

The extraction of metal ions on the modified silica was found to depend on the sorbate-sorbent characteristics as well as the experimental conditions. So the influence of the parameters on the metal extraction needed to be optimized for achieving the maximum extent of metal adsorption. In this thesis, five metal ions such as Co(II), Cu(II), Fe(II), Fe(III) and Mn (III), were used as target metals. The Schiff's base doped mesoporous silica which had the maximum amount of incorporated Schiff's base molecules were used as a sorbent in the extraction experiments. Some preliminary factors were evaluated in order to investigate the quantitative extraction. The pH of metal solution, the effect of salts present in metal solution, temperature and the amount of silica were the parameters studied. In addition, the selectivity of these modified silicas to various metal ions was evaluated. Finally, the desorption of metal from the silica using HNO_3 as desorption agents was studied.

4.4.1. Effect of pH of metal solution

The pH of metal solution was a crucial factor in the adsorption of metal because it could determine the values of the conditional stability constant of the metal complexes on the doping molecules in the modified silica. As reported by Boos and co-workers [48] that the addition of 0.1 M $NaNO_3$ into the metal solution increased the metal extraction capacity, so in this study all metal extraction experiments were studied using metal solution containing 0.1 M $NaNO_3$ in the pH range of 2.0-6.0 unless stated otherwise.

4.4.1.1. Extraction of Co(II)

The influence of pH on the extraction of Co(II) in the pH range of 2 to 5 was investigated. It was found that, for this pH range studied, only two mesoporous silica, non-doped and salen doped, were capable of extracting Co(II). The results were plotted between the amounts of Co(II) sorption and the initial pH of metal solution as shown in Figure 4.23.

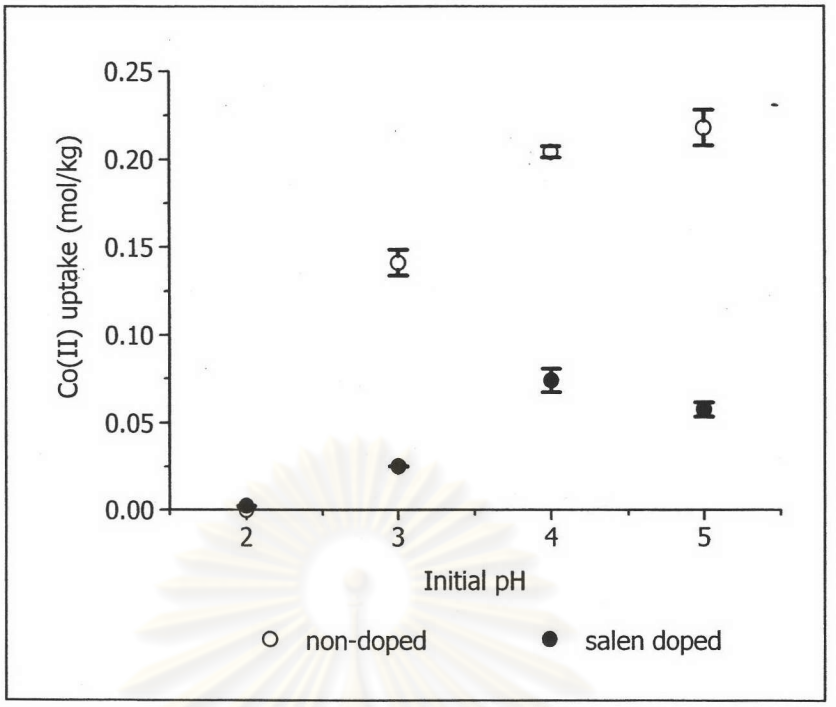

Figure 4.23 Effect of pH on Co(II) extraction properties of non-doped and salen doped mesoporous silica.

As shown in Figure 4.23, the non-doped mesoporous silica had more capacity to extract Co(II) than that of salen doped mesoporous silica. However, both silicas showed similar trend in extraction behavior. The amounts of the Co(II) extraction were lower at low pH, increased with the increasing of pH values and reached its maximum value around pH 4. The decrease amounts might be due to the competition between protons present in the solution and metal ions for retention on the sorbent. Thus, at low pH values, the metal extraction was hampered.

4.4.1.2. Extraction of Cu(II)

The preliminary study of Cu(II) extraction was performed using Cu(II) solution at pH 2. In this experimental condition, the lack of Cu(II) extraction ability for all mesoporous silica was observed. Further experiment was then conducted using Cu(II) solution at pH 3. During the extraction process, the precipitation of $Cu(OH)_2$ was formed. In fact, the pH of solution at equilibrium was about 6 which provoked facile precipitation. Hence, subsequent extraction test was carried out at pH 2.5. In this condition, the copper ions were not extracted by non-doped mesoporous silica. While all Schiff's base doped mesoporous silica were capable of extracting these ions. Actually, when the functionalized silica was mixed with the Cu(II) solution, the color

of silica was immediately changed to green which was the color of Cu-Schiff's base complex. The amounts of Cu(II) uptake by Schiff's base doped mesoporous silica from three replicated experiments was given in Table 4.21.

Table 4.21 The amounts of Cu(II) uptake by Schiff's base doped mesoporous silica.

Type of mesoporous silica	Cu(II) uptake	
	(mol/kg)	RSD(%)
Salen doped	0.1296 ± 0.0040	3.09
Saltn doped	0.1857 ± 0.0010	0.54
Salophen doped	0.1197 ± 0.0039	3.22
Haen doped	0.0448 ± 0.0046	4.78

From the results displayed in Table 4.21, the Cu(II) ions could be extracted quantitatively through all modified silica studied. The highest extracted value was obtained when saltn doped mesoporous silica was used as a sorbent, whereas haen doped mesoporous silica had the lowest Cu(II) extraction capacity. This highest extractability was probably due to the presence of the propyl group between two imine-N donor atoms on the structure of saltn. The propyl group offered these molecules the flexibility to behave like a tetradentate ligand and thus provided them the facility to form complex with metal. On the contrary, the lowest value of Cu(II) extraction might be explained in terms of structure of haen, which had methyl substituent groups on the imine-C atoms. These methyl groups caused steric hindrance occurred on the haen structure and had effect on the process of Cu(II) binding to the donor atoms of haen incorporated in silica. Therefore, the complexation ability on the process of Cu(II) with haen doped mesoporous silica was lower than those of other Schiff's base doped mesoporous silica.

4.4.1.3. Extraction of Fe(II)

In order to determine the effect of pH on the Fe(II) extraction efficiency of all materials, the pH of metal solution was varied from 2 to 6. The results were graphically demonstrated in Figure 4.24.

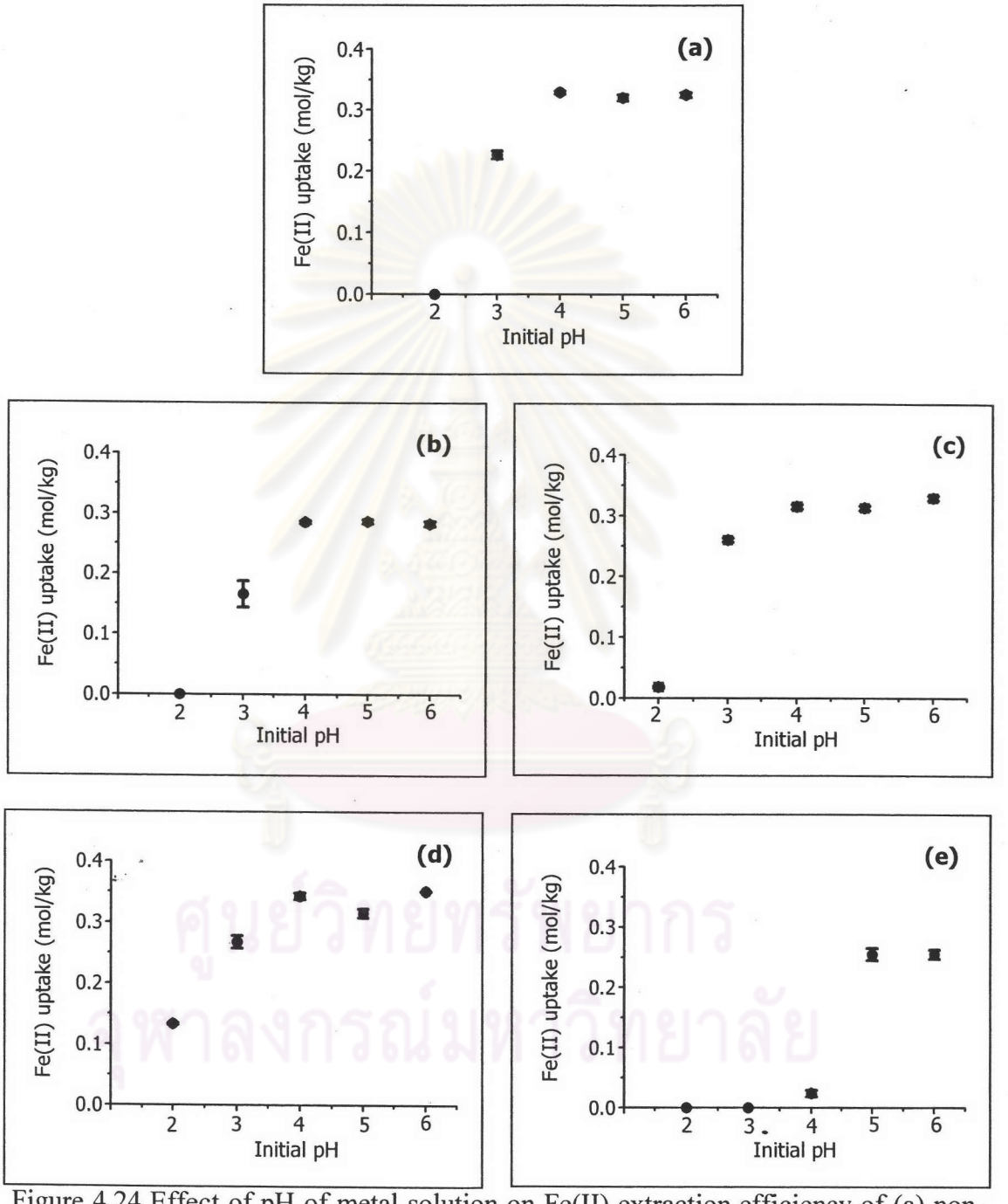

Figure 4.24 Effect of pH of metal solution on Fe(II) extraction efficiency of (a) non-doped, (b) salen doped, (c) saltn doped, (d) salophen doped and (e) haen doped mesoporous silica.

From Figure 4.24, it could be easily seen that Fe(II) extraction properties of all mesoporous silica had the same general trends. The sorption quantities of Fe(II) increased with the increasing of pH value and reached their maximum value around pH 4-5. However, after the extraction process the leaching of Schiff's base molecules out of silica was detected because the color of metal solution became brown which was the color of Fe(II)-Schiff's base complexes. Also, the leaching of such complexes was confirmed by the signal of UV absorbance at 278 nm. This seemed to be the reason for the very close extractability of Schiff's base doped mesoporous silica and non-doped mesoporous silica.

4.4.1.4. Extraction of Mn(II)

The effect of pH on the extraction of Mn(II) in the pH range of 2 to 6 was also studied. The experimental results showed that all types of modified silica did not extract any manganese ions in the pH range considerably. This behavior might be due to the inappropriate extraction condition used. Indeed, the preparation of Mn(II)-Schiff's base complexes were conducted at more severe condition such as higher temperature [63-65]. On the contrary, non-doped mesoporous silica had some capacity of Mn(II) extraction when the pH of metal solution was higher than 5. The amount of Mn(II) uptake was 0.0603 ± 0.0026 and 0.0659 ± 0.0034 mol/kg when the initial pH of metal solution were 5 and 6, respectively. However, as the Mn(II) extracted values was low, so these synthesized silica were not suitable for Mn(II) extraction, especially for the samples containing a lot of Mn(II) ions.

4.4.2. Effect of salts present in metal solution

As previously mentioned, the presence of 0.1 M $NaNO_3$ in metal solution played an important role in the extraction properties of mesoporous materials. And as we knew that the most abundant salt species in natural water were Na^+, K^+, Cl^- and NO_3^-. Therefore, the influence of these ions on the metal extraction properties were also investigated. The experiments were carried out using each metal solution containing various types of salts such as $NaNO_3$, NaCl, KNO_3 and KCl with 0.1 M in concentration. The results of each metal were described below.

4.4.2.1. Extraction of Co(II)

The influence of salts on Co(II) extraction was also studied using non-doped and Schiff's base doped mesoporous silica as sorbents. It was found that the haen doped mesoporous silica did not extract any Co(II) ions from all extraction condition used. The lack of Co(II) extractability may be caused by the haen structure. For other materials, their results were shown in Figure 4.25. The results given in this figure showed that all mesoporous silica had similar trends towards Co(II) extraction. Interestingly, for all silica, the amount of Co(II) uptake was higher when $NaNO_3$ was present in metal solution. This results seemed to be the advantage of these materials when applied for real sample containing several salts. However, the Co(II) extraction of most materials was relatively low comparing to other metal ions. Thus these materials may be not the appropriate sorbent for the application to the Co(II) extraction from samples containing immense amounts of Co(II).

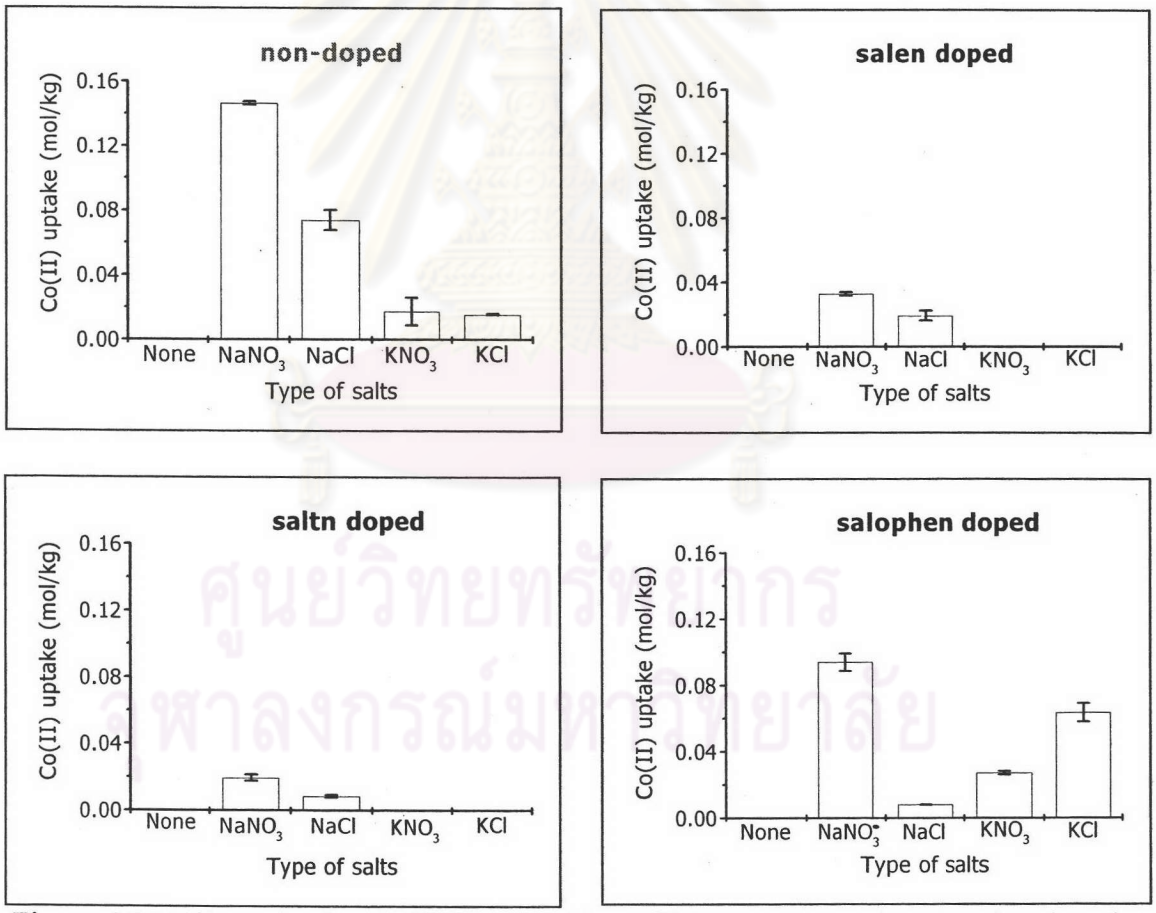

Figure 4.25 Effect of salts on Co(II) extraction efficiency of non-doped, salen doped, saltn doped, and salophen doped mesoporous silica.

4.4.2.2. Extraction of Cu(II)

The effect of salts on the Cu(II) extraction was conducted at pH 2.5. As described previously in section 4.4.1.2. that the non-doped mesoporous silica couldn't extract any Cu(II) ions in this condition, this effect of salts was then carried out on only four Schiff's base doped mesoporous silica. The amounts of Cu(II) uptake for each material were shown in Figure 4.26.

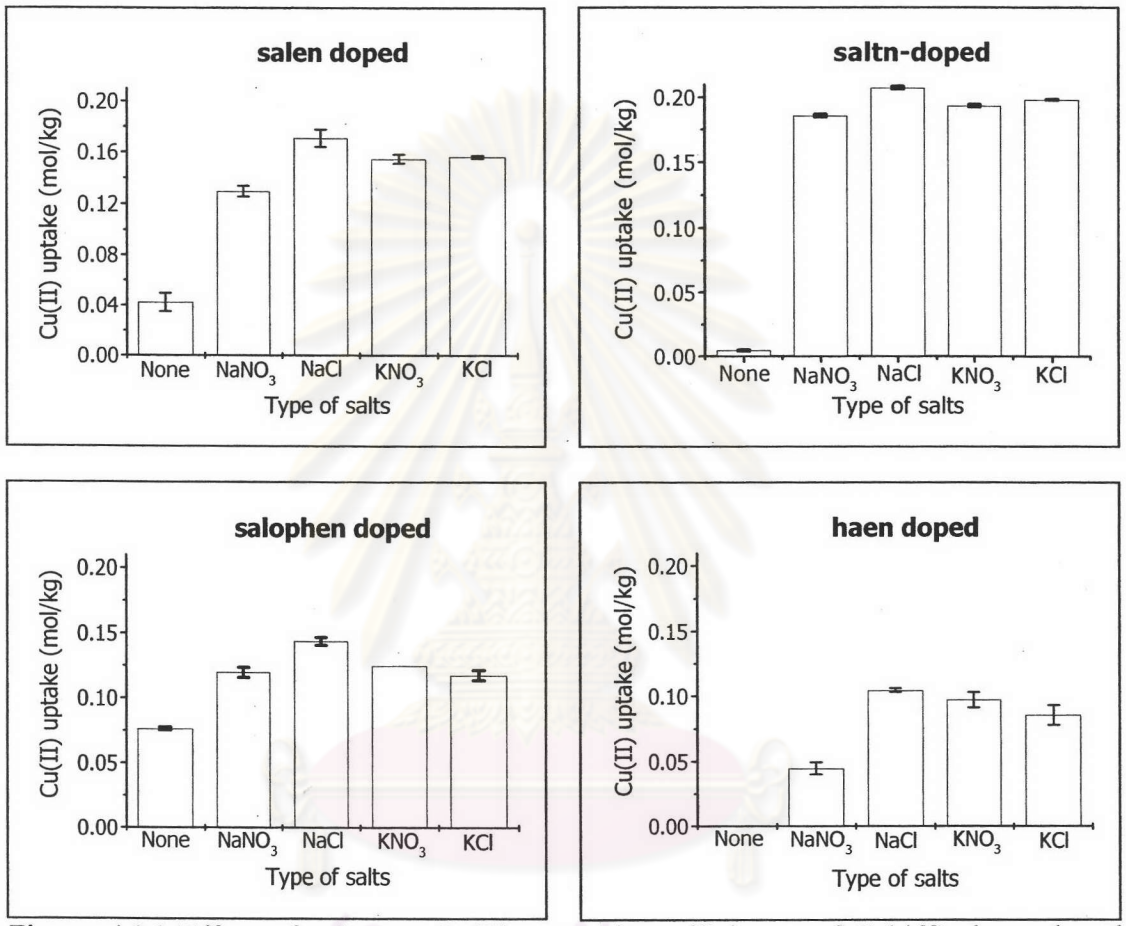

Figure 4.26 Effect of salts on Cu(II) extraction efficiency of Schiff's base doped mesoporous silica.

As could be seen in Figure 4.26, all Schiff's base doped mesoporous silica showed a similar trend towards Cu(II) extraction. In case of the absence of salt in the extraction system, the Cu(II) extracted values were generally low for all Schiff's base doped mesoporous silica used, especially for saltn doped and haen doped mesoporous silica. The presence of salt, especially NaCl, in metal solution augmented significantly the Cu(II) sorption capacity of materials. So, this result indicated the advantage of using the Schiff's base doped mesoporous silica as a sorbent for Cu(II) extraction when applied to real samples containing high saline (i.e. seawater). In addition,

among four Schiff's base doped mesoporous silica used as sorbent, the haen doped mesoporous silica showed the lowest extractability of Cu(II). This result seemed to be caused by the steric hindrance on its' structure as described previously.

4.4.2.3. Extraction of iron

4.4.2.3.1. Extraction of Fe(II)

The influence of salts on the Fe(II) extraction properties was performed at pH 4. The results of Fe(II) uptake in mol/kg were displayed in Figure 4.27. As could be seen in this figure, similar phenomenon comparing to other metal ions previously studied was observed. The presence of salts in solution enhanced the Fe(II) extraction capacity. However, the extractability of non-doped silica was slightly better than that of Schiff's base doped mesoporous silica. Lower extractability of the latter materials may be explained in terms of leaching of Schiff's base molecules during the extraction process. Indeed, the solution after extraction was brown in color which was the color of metal-Schiff's base complexes. The appearance of these complexes in solution was also confirmed by the peak occurred on UV-visible spectrum at 278 nm. Hence, all Schiff's base doped mesoporous silica were not suitable for the extraction of Fe(II) due to the decrease in lifetime of these materials after use.

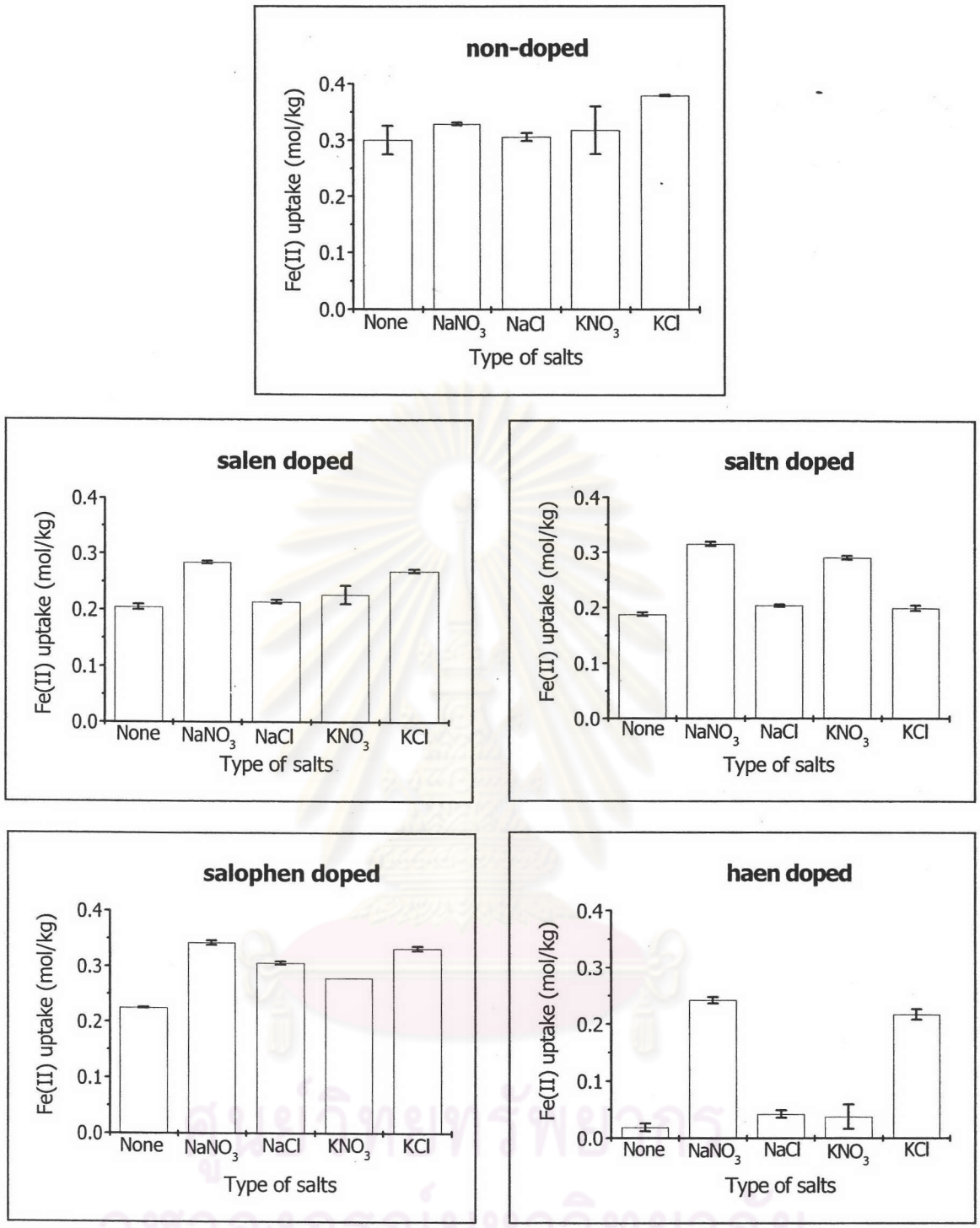

Figure 4.27 Effect of salts on Fe(II) extraction efficiency of non-doped and Schiff's base doped mesoporous silica.

4.4.2.3.2. Extraction of Fe(III)

For the extraction of Fe(III), only 0.1 M $NaNO_3$ was used as salt present in metal solution. The experimental results found that the non-doped mesoporous silica did not showed any extraction tendency towards Fe(III) ions in both two mediums studied. On the contrary, all Schiff's base doped mesoporous silica had the ability to

extract Fe(III) ions as shown in Figure 4.28. Thus, the Fe(III) extractability of these materials was likely due to the Schiff's base molecules inside the silica. This extraction behavior indicated the selectivity of Schiff's base doped mesoporous silica to the extraction of Fe(III).

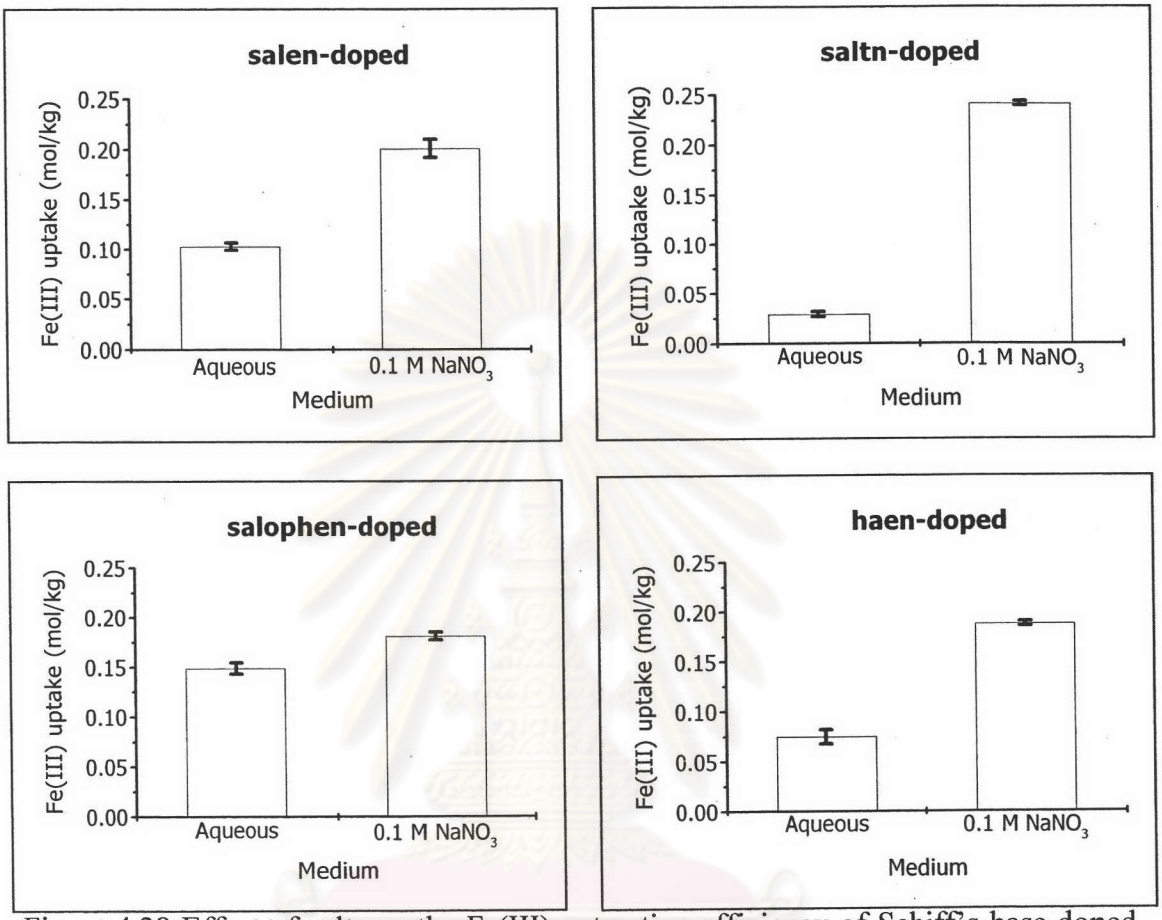

Figure 4.28 Effect of salts on the Fe(III) extraction efficiency of Schiff's base doped mesoporous silica.

The results given in Figure 4.28 displayed also the increase in Fe(III) extraction ability of all Schiff's base doped mesoporous silica when $NaNO_3$ was present in metal solution. Furthermore, among these materials, the saltn doped mesoporous silica had the highest Fe(III) extraction efficiency. This higher extracted value seemed to be originated mainly from the propyl groups on the saltn structure which had more influenced on the formation of 1 : 1 square-planar complex than respective ligands. This good extraction results was also considered as a favor of application of these materials to the determination of Fe(III) from waste water containing high saline.

4.4.2.4. Extraction of Mn(II)

The effect of salts on Mn(II) extraction properties of all modified mesoporous silica was also investigated. It was found that all synthesized mesoporous silica could not extract any Mn(II) ions in all conditions studied. Thus, it might be concluded that the non-doped and all Schiff's base doped mesoporous silica in this work were not the suitable sorbent for the extraction of Mn(II).

4.4.3. Effect of temperature

The effect of temperature was another factor that might be influenced on the metal retention efficiency of the sorbent. Thus, this effect should be opitimized to ensure quantitative retention of elements. The experiment was then carried out using two points of temperature, 25° and 40 °C. Salen doped mesoporous silica was used as a sorbent. Cu(II), Fe(III) and Mn(II) were chosen as sample ions. The medium used for each metal solution was 0.1 M NaCl at pH 2.5 for Cu(II), aqueous solution for Fe(III) and 0.1 M $NaNO_3$ for Mn(II). The selection of Cu(II) and Fe(III) was based on their higher extractability values compared to other metal ions studied. Also, Schiff's base doped mesoporous silica could extract more amounts of both metal ions than those of non-doped mesoporous silica. Consequently, these results indicated the selectivity of Schiff's base doped mesoporous silica towards Cu(II) and Fe(III) extraction. On the other hand, as Mn(II) could not be extracted in the entire conditions studied, so the effect of temperature was an interest factor to increase the Mn(II) extraction capacity of materials.

From the results, it was found that the functionalized silica could not extract any Mn(II) ions at both temperature studied. On the other hand, both Cu(II) and Fe(III) were found to be extracted by salen doped mesoporous silica and the extracted values were exhibited in Figure 4.29 below.

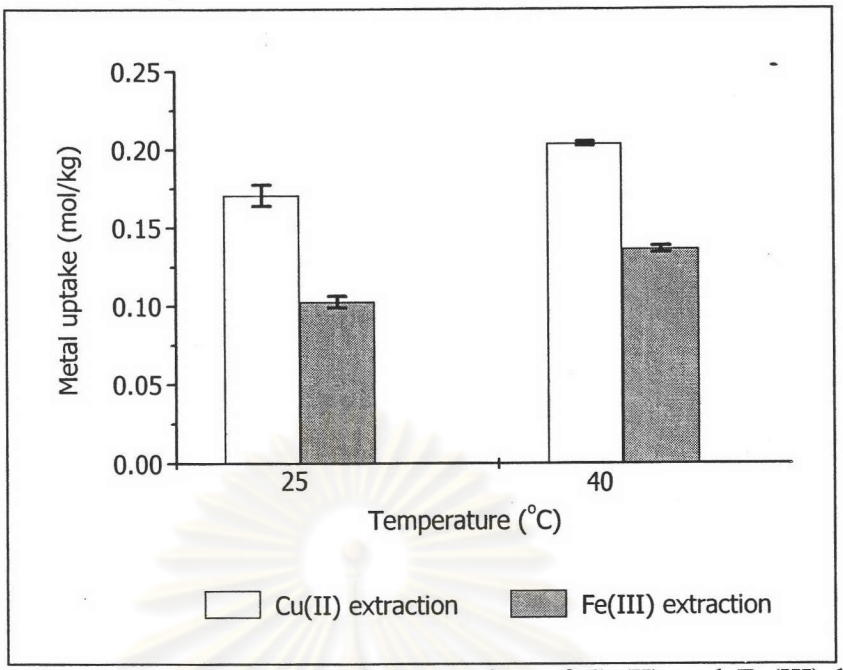

Figure 4.29 Effect of temperature on the extraction of Cu(II) and Fe(III) by salen doped mesoporous silica.

According to the extraction data from Figure 4.29, the amounts of Cu(II) and Fe(III) that could be extracted by salen doped mesoporous silica were affected by the temperature taken for the extraction process. The amounts of both extracted metals performed at 40 °C was higher than those carried out at 25 °C. However, the amount of Fe(III) extraction was lower than the Cu(II) extracted values. This results might be due to the occurrence of Fe(III)-salen complex in metal solution. Indeed, the black-brown color which was the color of this complex was observed in solution after extraction. The appearance of the Fe(III)-salen complex was also confirmed by the peak at 278 nm.

4.4.4. Effect of amount of silica

One of the key parameters in the evaluation of the metal extraction was the amount of sorbent. In order to elucidate the influence of this parameter, the experiment was carried out using Cu(II) solution in 0.1 M NaCl at pH 2.5 as a sample solution and the amount of all Schiff's base doped mesoporous silica was varied from 0.05 to 0.20 g. The extracted values of Cu(II) ions by different sorbents were plotted as a function of amount of silica as displayed in Figure 4.30.

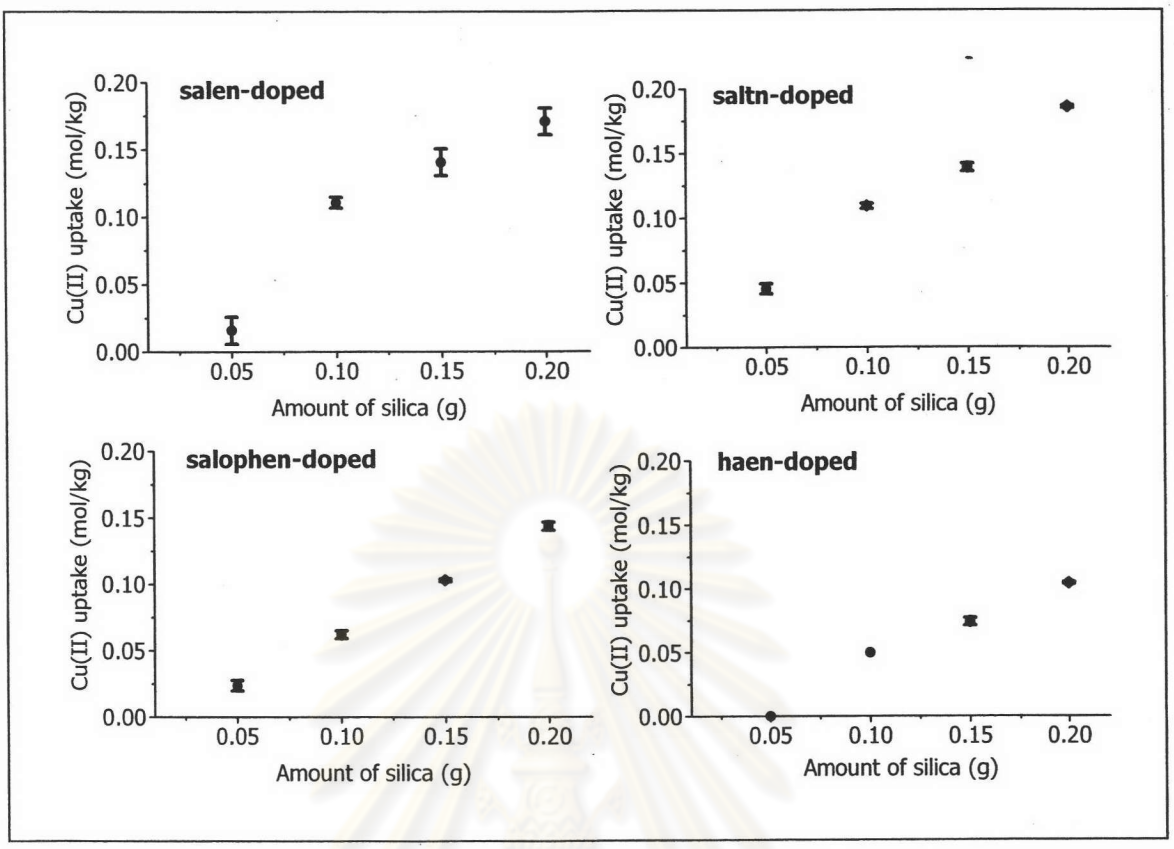

Figure 4.30 Effect of amount of Schiff's base doped mesoporous silica on the amount of Cu(II) extraction.

As seen from Figure 4.30, similar trend of Cu(II) uptake was obtained from all Schiff's bases doped mesoporous silica. When the amount of silica changed to higher values, the amount of Cu(II) extraction was significantly increased. The maximum of the Cu(II) uptake was obtained when the amount of sorbent was maximized (*i.e.* 0.20 g in this case).

4.4.5. Determination of Cu(II) extraction capacity

The determination of Cu(II) extraction capacity was conducted in order to compare the sorption properties of each Schiff's base doped mesoporous silica. The medium of Cu(II) solution used in this study was pH 2.5 with the presence of NaCl. The concentration of Cu(II) was varied from 50 to 200 ppm. The obtained results of Cu(II) extraction capacity of each materials were presented in Figure 4.31.

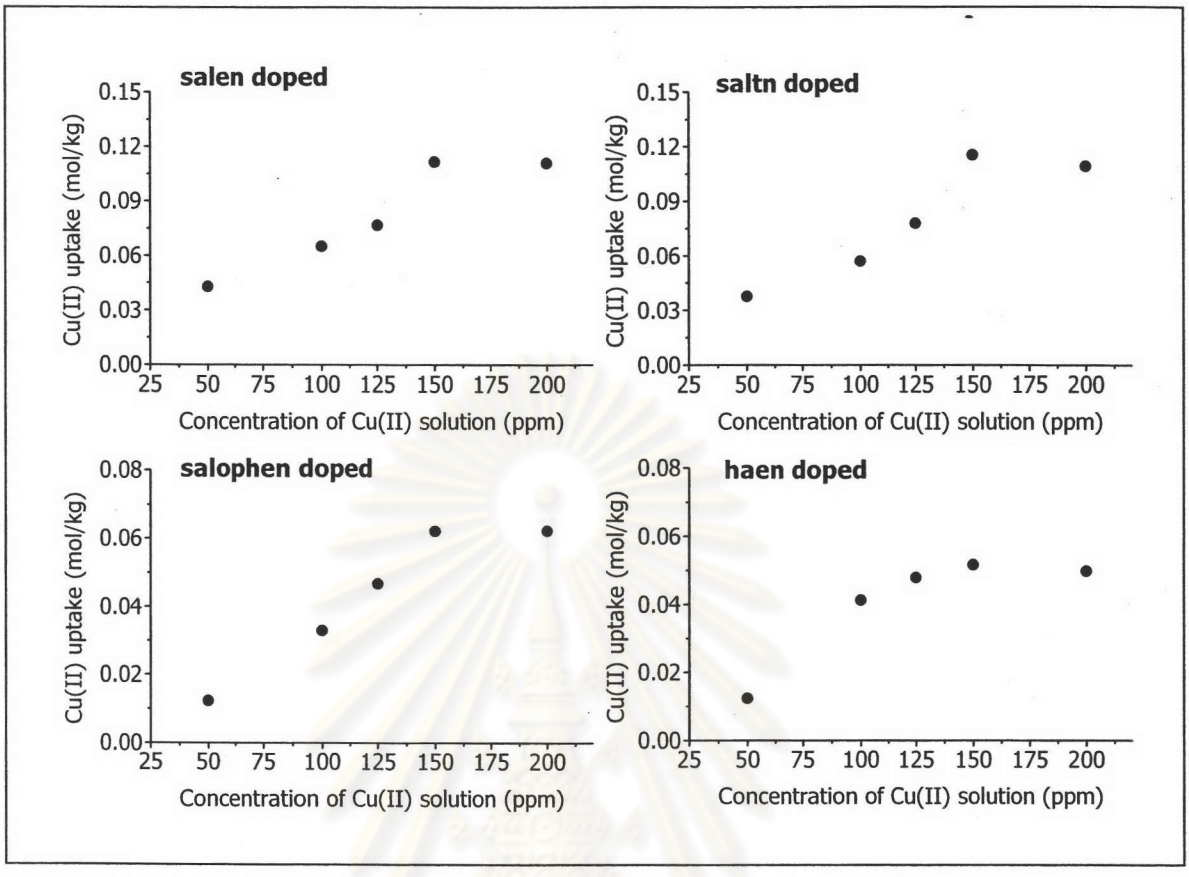

Figure 4.31 The Cu(II) extraction capacity of each mesoporous silica as a function of Cu(II) concentration.

From Figure 4.31, the Cu(II) extractability of all Schiff's base doped mesoporous silica seemed to be increased with the increasing of Cu(II) concentration. The maximum uptake of Cu(II) was obtained when the concentration of this metal was equal or more than 150 ppm. Considerring the Cu(II) adsorption ability of the doping materials, it was found that the salen and saltn doped mesoporous silica had better extractability than the salophen and haen doped mesoporous silica. In addition, from the relation between the amounts of Cu(II) uptake and those of incorporated Schiff's bases as shown in Table 4.22, it could be concluded that the Cu(II) extraction capacity of Schiff's base doped mesoporous silica was found to be in this sequence: saltn > salen > salophen > haen doped mesoporous silica. The highest Cu(II) uptake of saltn doped mesoporous silica was probably based on the facility of this Schiff's bases to act as a tetradentate ligand and hence promoted the formation of saltn-metal complex.

Table 4.22 Ralation between the amounts of Cu(II) uptake and those of incorporated Schiff's bases.

Type of silica	Incorporated Schiff's bases (μmole)	Cu(II) uptake (μmole)	Schiff's bases : Cu(II) uptake (mole ratio)
Salen doped	66.7	12.2	1 : 0.17
Saltn doped	35.3	11.5	1 : 0.33
Salophen doped	46.6	6.30	1 : 0.14
Haen doped	51.2	5.20	1 : 0.10

4.4.6. Desorption

In order to determine the reusability of the synthesized mesoporous silica, the desorption of metal adsorbed on the modified mesoporous silica was becoming an interesting study. According to previous results, all Schiff's base doped mesoporous silica is favorable for the extraction of Cu(II) and Fe(III). Also, the extraction amounts of both metals were higher than those of other metal ions studied. Therefore, the desorption of these two ions was initiated using nitric acid as a desorption agent. The reason for the choice of this acid was that nitrate ion was reported to be more acceptable matrix for both flame and electrothermal AAS experiments than chloride ion and sulfate ion [66]. Three different concentrations of nitric acid such as 0.01, 0.05 and 0.1 M were applied. The Cu(II) desorption study was performed on the silica which had extracted Cu(II) at pH 2.5 in the presence of $NaNO_3$ or NaCl. For the Fe(III) desorption, the silica which had extracted Fe(III) from aqueous solution with the presence or absence of $NaNO_3$ were used. The desorption results for Cu(II) and Fe(III) ions expressed in percentage were displayed in Figure 4.32 and Figure 4.33, respectively.

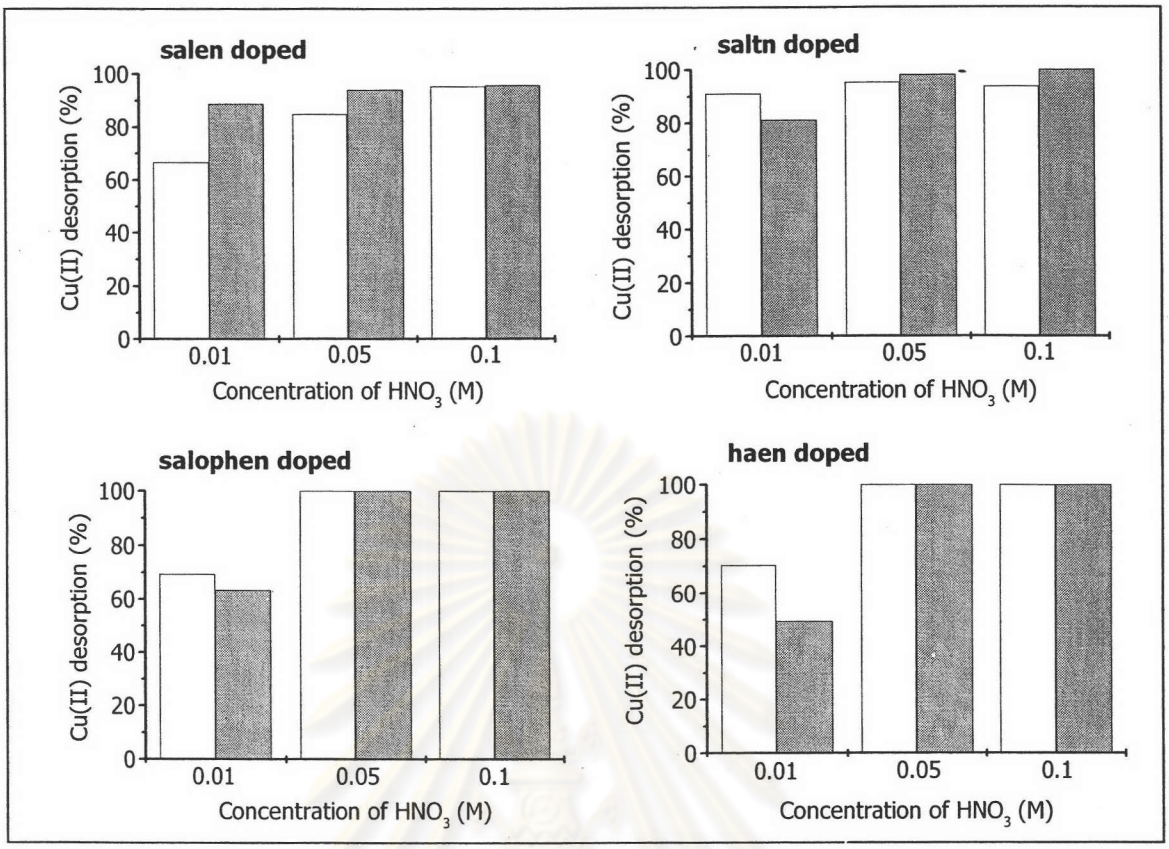

Figure 4.32 Effect of HNO_3 concentration on the desorption of Cu(II) ion from each of Schiff's base doped mesoporous silica which had extracted Cu(II) at pH 2.5 in the presence of: □, $NaNO_3$; ▩, NaCl.

From Figure 4.32, the Cu(II) ions were completely released from all doping materials when the concentration of HNO_3 was equal or more than 0.05 M. On the contrary, when 0.01 M HNO_3 was used, the moderately desorption of Cu(II) was observed. Considering the effect of adsorption medium on the desorption of Cu(II), similar results were observed for both mediums used. It was thus implied that the adsorption medium had no effect on the Cu(II) desorption efficiency.

For the Fe(III) desorption, the results were shown in Figure 4.33. As seen from this figure, the Fe(III) desorption was completely achieved when 0.1 M HNO_3 was applied. This result suggested that the desorption of Fe(III) required more violent condition than that of Cu(II). For the effect of adsorption medium on the desorption of Fe(III), different desorption results were observed between both mediums when the concentration of nitric acid was less than 0.1 M. The percentage of Fe(III) desorption from Schiff's base doped mesoporous silica which had extracted these metal ions from aqueous solution with the presence of $NaNO_3$ was less than that

from aqueous solution. This phenomenon indicated the effect of adsorption medium on the Fe(III) desorption efficiency, especially when the low concentration of desorpting agent was used.

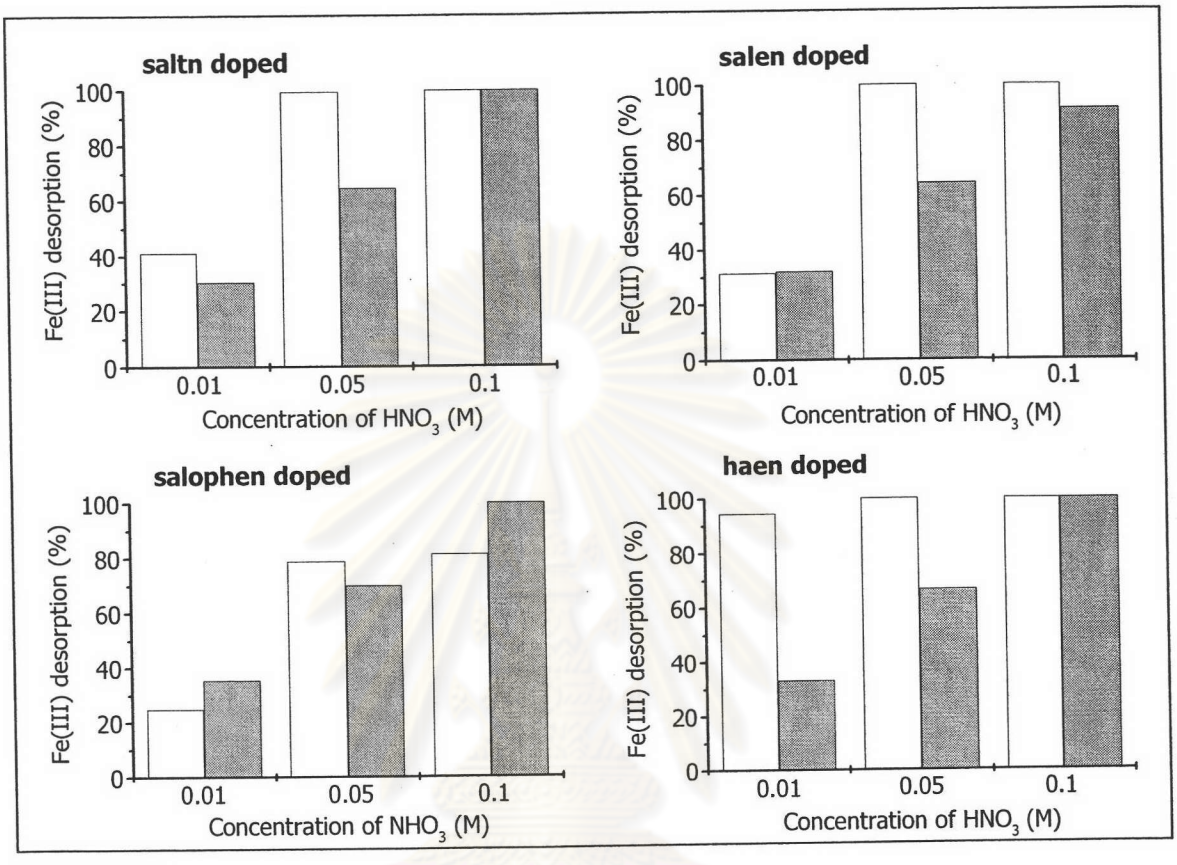

Figure 4.33 Effect of HNO_3 concentration on the desorption of Fe(III) ion from each of Schiff's base doped mesoporous silica which had extracted Fe(III) from aqueous solution with: □, absence $NaNO_3$; ▨, presence $NaNO_3$.

4.4.7. Selectivity of materials to metal extraction

From previous sections, among several metal ions studied, only Cu(II) and Fe(III) ions were found to be extracted by the synthesized Schiff's base doped mesoporous silica. Therefore, these metal ions were selected for the study of materials' selectivity to extraction. The results of metal extracted values expressed in mol/kg from three replicate experiments were exhibited in Table 4.23.

Table 4.23 The amounts of Cu(II) and Fe(III) extracted from binary mixture by different kinds of mesoporous silica.

Type of mesoporous silica	Metal uptake (mol/kg)	
	Cu(II)	Fe(III)
Non-doped	0	0
Salen doped	0	0.1823 ± 0.0006
Saltn doped	0	0.1988 ± 0.0025
Salophen doped	0.0204 ± 0.0010	0.1985 ± 0.0011
Haen doped	0	0.1732 ± 0.0080

From Table 4.23, it could be concluded that non-doped mesoporous silica did not extract any Cu(II) and Fe(III) ions. These results were in accordance with the aforementioned extraction studies. Considering the Schiff's base doped mesoporous silica, the difference in the Cu(II) and Fe(III) extraction behavior clearly demonstrated the strong selectivity of Schiff's base doped mesoporous silica to Fe(III) extraction. The great selectivity of these doping silica to the extraction of Fe(III) will be of benefit to the extraction of this ion not only from binary mixture containing Cu(II) but also from sample containing other metal ions without significant interference.